NAVAL POSTGRADUATE SCHOOL

MONTEREY, CALIFORNIA

THESIS

A NOVEL NONELECTROLYTIC PROCESS FOR CHROMIUM AND NICKEL COATING

by

Karima A. Greenaway

June 2015

Thesis Advisor: Jonathan Phillips
Co Advisor: Claudia C. Luhrs

Approved for public release; distribution is unlimited

THIS PAGE INTENTIONALLY LEFT BLANK

REPORT DOCUMENTATION PAGE			Form Approved OMB No. 0704–0188

Public reporting burden for this collection of information is estimated to average 1 hour per response, including the time for reviewing instruction, searching existing data sources, gathering and maintaining the data needed, and completing and reviewing the collection of information. Send comments regarding this burden estimate or any other aspect of this collection of information, including suggestions for reducing this burden, to Washington headquarters Services, Directorate for Information Operations and Reports, 1215 Jefferson Davis Highway, Suite 1204, Arlington, VA 22202-4302, and to the Office of Management and Budget, Paperwork Reduction Project (0704-0188) Washington, DC 20503.

1. AGENCY USE ONLY (Leave blank)	2. REPORT DATE June 2015	3. REPORT TYPE AND DATES COVERED Master's Thesis	
4. TITLE AND SUBTITLE A NOVEL NONELECTROLYTIC PROCESS FOR CHROMIUM AND NICKEL COATING		5. FUNDING NUMBERS	
6. AUTHOR(S) Karima A. Greenaway			
7. PERFORMING ORGANIZATION NAME(S) AND ADDRESS(ES) Naval Postgraduate School Monterey, CA 93943-5000		8. PERFORMING ORGANIZATION REPORT NUMBER	
9. SPONSORING /MONITORING AGENCY NAME(S) AND ADDRESS(ES) N/A		10. SPONSORING/MONITORING AGENCY REPORT NUMBER	

11. SUPPLEMENTARY NOTES The views expressed in this thesis are those of the author and do not reflect the official policy or position of the Department of Defense or the U.S. Government. IRB Protocol number ____N/A____.

12a. DISTRIBUTION / AVAILABILITY STATEMENT Approved for public release; distribution is unlimited	12b. DISTRIBUTION CODE

13. ABSTRACT (maximum 200 words)

The use of hexavalent chromium in metal coating operations, as per electrolytic processing, is subject to increasingly restrictive regulations due to its carcinogenic and toxic properties. Yet, these coatings are critical for corrosion resistance in aircraft parts such as hydraulic systems. This has led to many efforts to find high quality "non-electrolytic" coating processes. The guiding hypothesis of this work was that a version of the Reduction Expansion Synthesis (RES) process, previously used to produce submicron metal particles, could be developed to create metal coating. This study involved the production of coatings by a variety of RES-like protocols, based on mixing metal nitrates, urea, and sometimes other reagents with uncoated metal wires, then heating (ca. 900 C) in an inert atmosphere. The primary tools employed to study the coatings were optical microscopy, x-ray diffraction, scanning electron microscope, and energy dispersive x-ray microprobe. The first protocol created essentially a carbon surface layer. This was mitigated in later protocols, and the coatings contained the desired metals. However, the coating morphology was imperfect and contained impurities. Clearly, metal can be deposited with RES like processes, but further development will be needed to create metal layers of acceptable quality.

14. SUBJECT TERMS Reduction Expansion Synthesis (RES), metal coating, chrome coating, nickel coating	15. NUMBER OF PAGES 105
	16. PRICE CODE

17. SECURITY CLASSIFICATION OF REPORT Unclassified	18. SECURITY CLASSIFICATION OF THIS PAGE Unclassified	19. SECURITY CLASSIFICATION OF ABSTRACT Unclassified	20. LIMITATION OF ABSTRACT UU

NSN 7540–01-280-5500

Standard Form 298 (Rev. 2–89)
Prescribed by ANSI Std. 239–18

THIS PAGE INTENTIONALLY LEFT BLANK

A NOVEL NONELECTROLYTIC PROCESS FOR CHROMIUM AND NICKEL COATING

Karima A. Greenaway
Lieutenant, United States Coast Guard
B.S., United States Coast Guard Academy, 2005

Submitted in partial fulfillment of the
requirements for the degree of

MASTER OF SCIENCE IN MECHANICAL ENGINEERING

from the

NAVAL POSTGRADUATE SCHOOL
June 2015

Author: Karima A. Greenaway

Approved by: Jonathan Phillips
                Thesis Advisor

                Claudia C. Luhrs
                Co-Advisor

                Garth V. Hobson
                Chair, Department of Mechanical and Aerospace Engineering

THIS PAGE INTENTIONALLY LEFT BLANK

ABSTRACT

The use of hexavalent chromium in metal coating operations, as per electrolytic processing, is subject to increasingly restrictive regulations due to its carcinogenic and toxic properties. Yet, these coatings are critical for corrosion resistance in aircraft parts such as hydraulic systems. This has led to many efforts to find high quality "non-electrolytic" coating processes. The guiding hypothesis of this work was that a version of the Reduction Expansion Synthesis (RES) process, previously used to produce submicron metal particles, could be developed to create metal coating. This study involved the production of coatings by a variety of RES-like protocols, based on mixing metal nitrates, urea, and sometimes other reagents with uncoated metal wires, then heating (ca. 900 C) in an inert atmosphere. The primary tools employed to study the coatings were optical microscopy, X-ray diffraction, scanning electron microscope, and energy dispersive X-ray microprobe. The first protocol created essentially a carbon surface layer. This was mitigated in later protocols, and the coatings contained the desired metals. However, the coating morphology was imperfect and contained impurities. Clearly, metal can be deposited with RES like processes, but further development will be needed to create metal layers of acceptable quality.

THIS PAGE INTENTIONALLY LEFT BLANK

TABLE OF CONTENTS

LIST OF FIGURES

LIST OF TABLES

THIS PAGE INTENTIONALLY LEFT BLANK

LIST OF ACRONYMS AND ABBREVIATIONS

μm	Micrometer/Microns
AWG	American wire gauge
Cr	chromium
DOD	Department of Defense
EPA	Environmental Protection Agency
Fe	iron
mm	millimeter
Na_2CO_3	Sodium Carbonate Monohydrate
Ni	nickel
nm	nanometer
OSHA	Occupational Safety and Health Administration
PVD	Physical Vapor Deposition
RES	Reduction Expansion Synthesis
rpm	revolutions per minute
sccm	standard cubic centimeter per minute
SEM	Scanning Electron Microscopy
TEM	Transmission Electron Microscope
XRD	X-Ray Diffractometry/Diffractometer

THIS PAGE INTENTIONALLY LEFT BLANK

ACKNOWLEDGMENTS

THIS PAGE INTENTIONALLY LEFT BLANK

I.   INTRODUCTION

This chapter provides an overview of the benefits of commercial metal coating techniques and highlights the harmful qualities that sparked our interest in pursuing this area of study. Of particular concern is that while metal plating processes have been around for decades, so have the serious human and environmental dangers that are negative consequences of these production methods. Namely, the use of hexavalent chromium (CrVI) in electrolytic coating techniques, long regarded as the premier means for preventing wear and corrosion of some metals is now strictly minimized and highly regulated by government agencies for its toxicity. These restrictions are also affecting the ability of the Department of Defense (DOD) to maintain mission ready and capable assets, as it struggles to identify environmentally friendly coating alternatives that offer the same or better performance parameters.

A.   OVERVIEW

Metal coating, commonly referred to as surface finishing, is one of the oldest innovations known for enhancing the form and function of the material it protects. It can be used as a surface protectant on metallic and non-metallic objects called substrates. Its long history has played a major role in community infrastructures around the world, influencing practically every industry available, and increasing the overall quality of life for millions.

Two of the most widely used metal finishing are arguably chromium (chrome) plating and nickel plating. These coating techniques create hard, corrosion-resistant, durable surfaces in various non-engineering and engineering applications. Such techniques are critical from a military standpoint given, for example, that U.S. Navy aircraft carriers experienced failures of the aircraft launching system within a year of service as a result of wear and corrosion [1]. Furthermore, as detailed elsewhere [1], the dramatic improvement to the service life as a result of electroless nickel coating being applied to the aircraft catapult covers. This particular example illustrates the huge benefits of metal coating applications to the operational capability and reliability of the

military's aircraft launching mechanism. Meanwhile, chrome plating in the form of hexavalent chromium (CrVI) has been regarded as the "gold standard" against corrosion in military applications for decades [2]. Its uses range from electronics to aircrafts components.

While metal coatings have advanced the dependability and durability of many systems, certain coating application processes have raised concerns and drawn criticism for their adverse effects. Specifically, chrome coating is problematic as it involves electrolytic (high current) coating in extremely low pH acid baths using highly toxic chrome precursors [3, 4]. For these and other reasons, there is a push to find greener alternatives or suitable replacements for existing coating processes that pose substantial environmental risks [2-5].

B.   HISTORY

The earliest civilizations harnessed applications of metal coating in an effort to decorate and preserve artifacts. Ingo et al. researched plating methods used by early craftsmen [6]. They recorded that mercury silvering and gilding techniques were used at that time to cover metal objects with thin sheets of silver or gold. Furthermore, these researchers discovered that for centuries, the metal plating industry was dominated by mercury-based coating methods because of their relatively low cost and aesthetic appeal. By the mid-1800s, electroplating techniques were introduced and eventually, they outperformed these mercury-based methods [6]. At that time, electroplating was easily scalable and revolutionized the industry at a time when mercury was exposed for its toxicity [6]. In time, mercury-based coating techniques were virtually discontinued because they grew to be more expensive due to their harmful risks.

Today, there are a growing number of metal coating/plating techniques available for commercial use. These include, but are not limited to, the following: electroplating, sputtering, thermal spraying, and plasma spraying [7]. Chrome and/or nickel coatings are typically applied by one of these methods. Consumers weigh performance and life-cycle costs when choosing the best product for the application, however, it is also equally important to calculate the risks.

1.   Electroplating

Electroplating occurs by immersing a conductive metal in an aqueous solution of the coating metal and supplying the cell with an electrical current [8, 9]. The material being coated serves as the cathode also referred to as the negative electrode. The anode consists of either the same metal in the aqueous solution or a chemically inactive metal, like copper or platinum, used only as a path for the electrons to flow [9]. The metal to be coated becomes negatively charged and attracts the positively charged ions in the solution, which triggers the electrodeposition of the coating onto the surface of the material.

Chrome electroplating is illustrated in Figure 1, which depicts an unknown component cathode and a lead (Pb) anode connected to a power source and submerged in a plating bath containing chromium trioxide (CrO_3) and sulfuric acid (H_2SO_4) [10]. The positively charged Cr ions from the solution are attracted to the negatively charged component and deposit onto the surface, creating a chrome coating [10]. Toxic CrVI mist is emitted into the environment from the plating bath. Hazardous byproducts including sludge and contaminated parts collect in the tank, all of which require special handling and disposal [10].
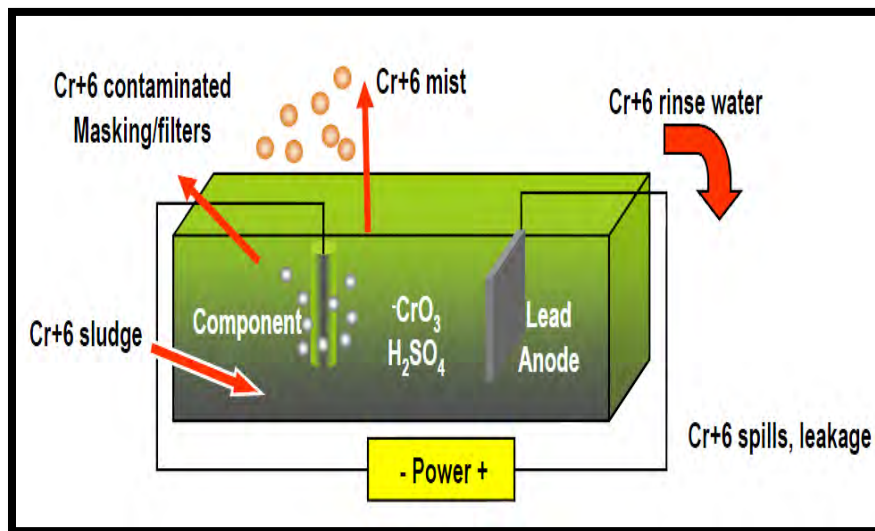
Figure 1.   Chrome electroplating uses chromic acid solutions to apply coatings with thicknesses between 0.001" to 0.015," from [10].

3

Decorative electrodeposition of nickel is usually done in conjunction with a chrome overlay, Ni-Cr coating [11]. Recently, Ni-Cr plating has seen improved corrosion protection with the development of a microdiscontinuous chromium layer to combat surface porosity normally affecting the Cr topcoat (see Figure 2) [11, 12]. As detailed elsewhere [12], microdiscontinuous chromium protects steel, zinc, copper, aluminum, and other materials. Nickel coatings used in engineering applications offer similar protection and pollution challenges to chrome coating, the difference being that nickel coating processes have mostly transitioned to cleaner alternatives. As such, nickel coating processes using non-electrolytic techniques are now widely employed; meanwhile chrome coating is still almost universally applied via electrolytic methods. The use of some metals in electroplating such as cadmium and lead however, are restricted by the Environmental Protection Agency (EPA) due to their toxic quality [7].
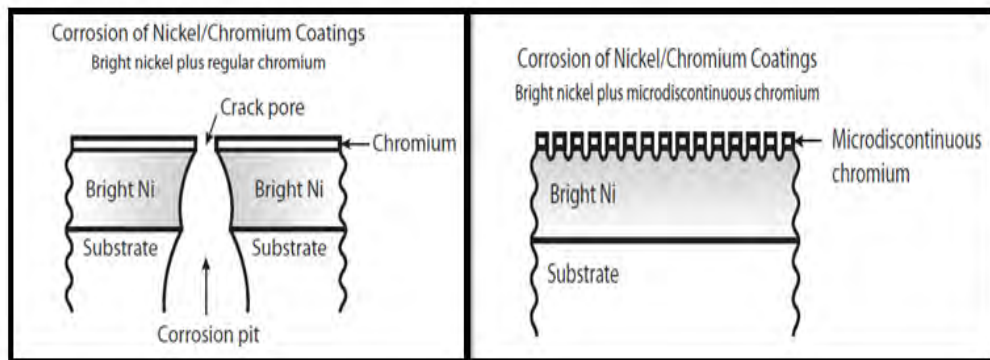
Figure 2.   Nature on corrosion pitting on: (left) single-layer nickel plus
chromium and (right) microdiscontinuous chromium over nickel,
from [11]

Lou et al. [9] describe the electroplating treatment process as involving immersion of the material being coated in a series of baths, outlined in Figure 3. They further indicate that specific chemical compositions of electroplating baths are mostly proprietary but the fundamentals of electroplating are geared towards the same results—bolstering surface appearance, providing protection, or enhancing material properties.
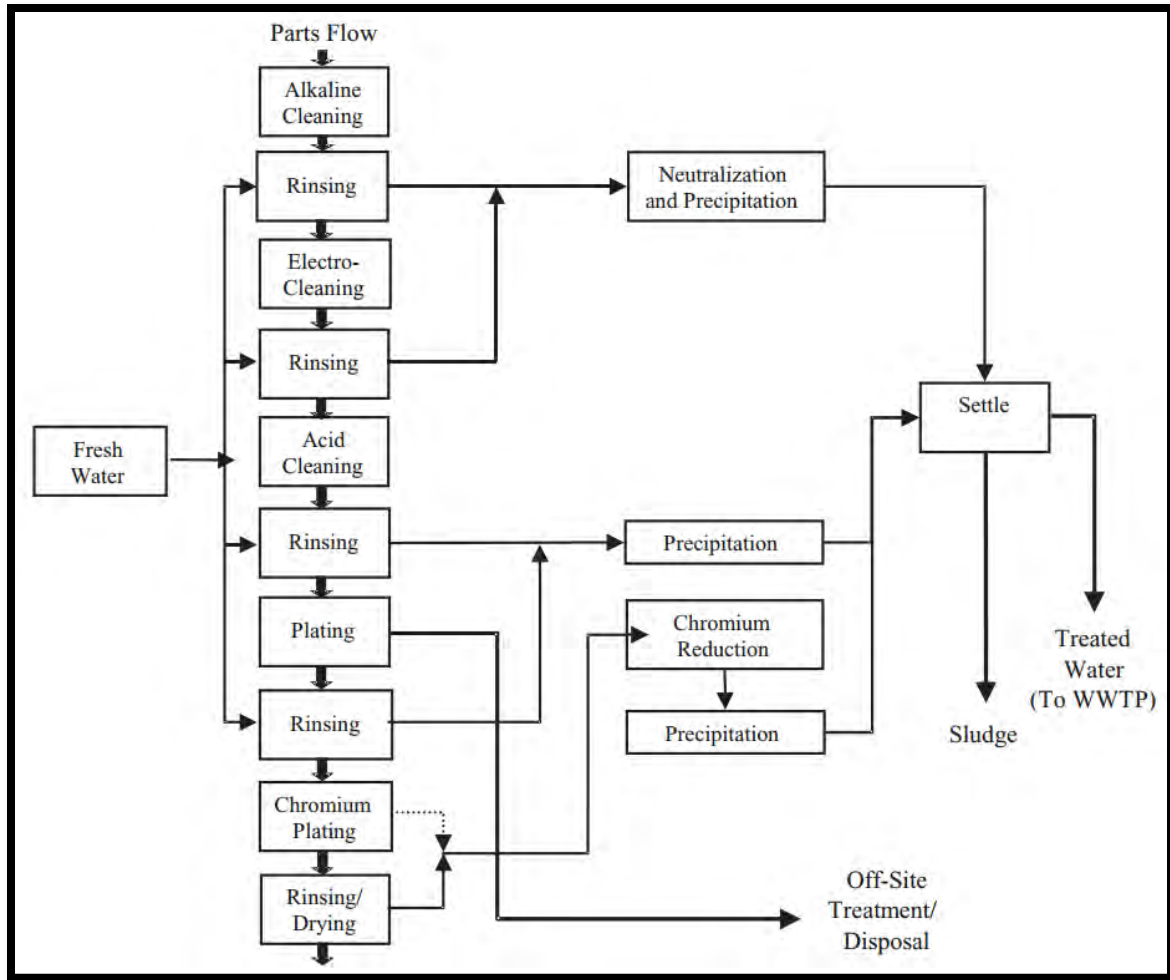
Figure 3.   Electroplating process flow chart, from [9].

Today, electroplating continues to be one of the leading metal coating techniques despite a growing demand for technological advances to eliminate the adverse effects associated with its use. Manufacturers employing this coating method are now burdened with meeting and maintaining compliance with Occupational Safety and Health Administration (OSHA) and Environmental Protection Agency regulations for worker safety and pollution prevention [2, 3].

2.   Electroless plating

Electroless plating is an autocatalytic coating technique that results from a controlled chemical reaction between a metal substrate and a reducing agent [13, 14]. The

main difference between electroless plating and electroplating is that metal deposition is not driven by current source. The absence of a current flow permits a constant deposition rate throughout the coating process, which is directly responsible for the thickness uniformity on complex surface geometries [13, 14]. According to [13, 14], major advantages of electroless plating over other techniques include uniform coating distribution illustrated in Figure 4, less porosity which increases the effectiveness of the protective layer, and reduced energy consumption through the absence of an external power supply.
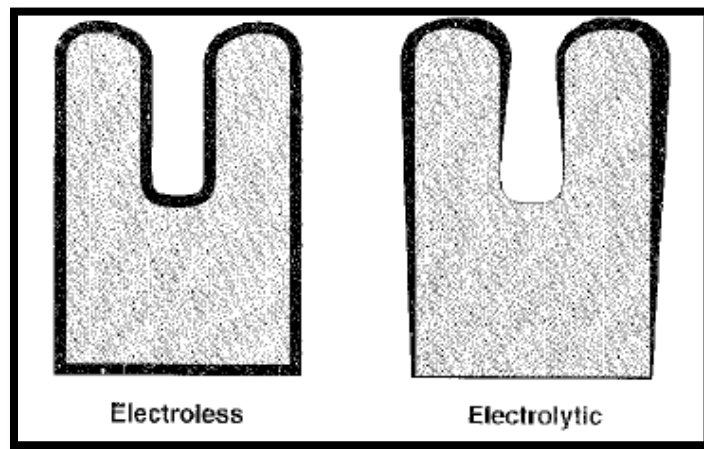
Figure 4.   The constant deposition rate in electroless nickel plating techniques
produces a uniform coating thickness on complex surfaces,
from [14].

Schlesinger [13] describes the electroless deposition process illustrated in Figure 5 as following follows two different methods. One plating sequence includes solutions to sensitize and catalyze the metal to be coated. The alternate plating sequence includes a catalyzing solution with a mixed colloid followed by an activation process to remove unwanted surface layers formed by interaction of stabilizers in solution. A material is treated with either the first or the second electroless plating bath sequence based on the inherent behavioral properties of the substrates in solution [14]. As discussed in detail elsewhere [15], electroless plating has not been perfected for use with chrome plating

applications, in particular on a steel substrate, due to susceptibility of the electroless plating bath to become contaminated.
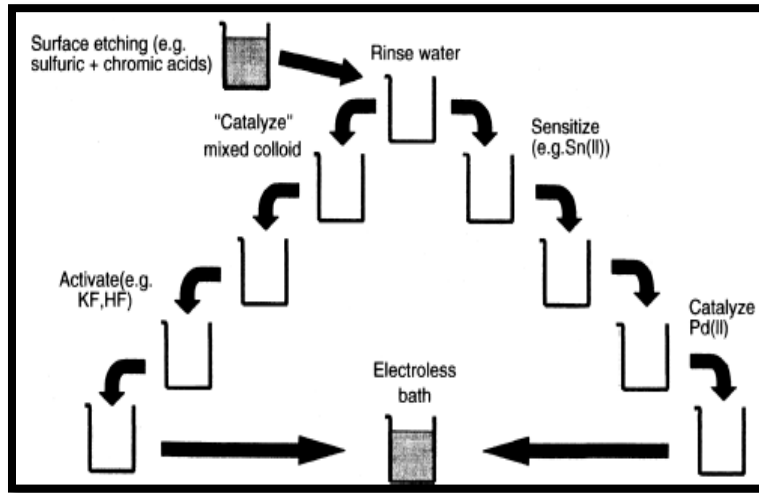
Figure 5.   Electroless deposition schematic, from [13].

3.   Sputtering

Sputtering is a PVD process that results when a high temperature or inert gas is supplied to a vacuum chamber containing a target material and a substrate [7, 16, 17]. Highly accelerated Argon ions hit a target surface, transferring significant kinetic energy to atoms on the surface. This causes the surface atoms to "sputter," that is, they leave the surface, very energetically, and freeze when they hit a cold surface and condense as illustrated in Figure 6 [16, 17]. The geometry of the system determines how many of the sputtered atoms hit the substrate. The positioning of the substrate within the chamber allows for one side to be coated at a time.

7
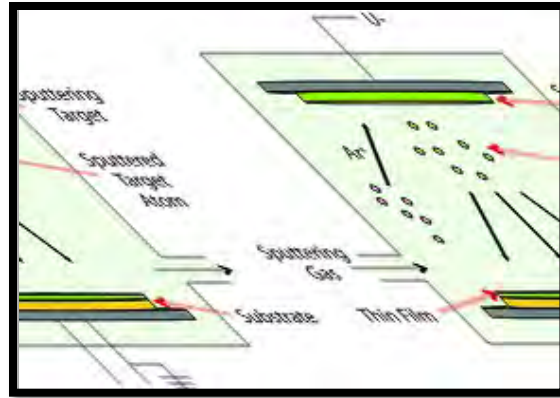
Figure 6. Sputtering deposition process, from [17].

Based on [17], some advantages with the use of this technique include infinite substrate options, no unwanted alteration of substrate properties, thickness uniformity on the plate being coated, low costs, low energy, and no pollution. The sputter deposition coating method is commonly used for developing thin films in integrated circuits, but has seen commercial use in chrome plating applications. Indeed, it is not appropriate for large substrates as the cost of the matching large vacuum chambers and associated pumps is prohibitive.

4.   **Thermal spraying**

Thermal spraying utilizes a gun that sprays liquefied coating material onto a roughened metal surface [7]. Reeve [18], suggested that concurrent coating of several components is possible, while a vacuum chamber is typical for spraying smaller pieces in order to prevent impurities on the surface layer. Zinc and aluminum are commonly used as coating metals with this technique on iron substrates [7]. Additionally, thermally sprayed Ni-Cr alloy is applied to on metals with operating temperatures around 1800°F [7]. There are a few limitations associated with its use that include "line-of-site" surfaces and uneven coating thicknesses due to surface contours [18]. This technology is commonly used in the aerospace industry to provide wear, corrosion, and thermal resistance in aircraft systems.

5. Plasma spraying

Plasma spraying is a form of thermal spraying and involves similar protocols for coating an object. The process proceeds after powder is injected into a plasma jet then superheated before being sprayed onto the substrate through a high velocity plasma torch as shown in Figure 7 to create millimeter-thick coatings [7, 19, 20]. The high kinetic energy of the propelled atoms causes the strong bonding with the surface, ultimately producing corrosion and wear-resistant parts for high temperature operations [7, 19, 20]. It is widely used in aircraft engine components, particularly turbine blades.
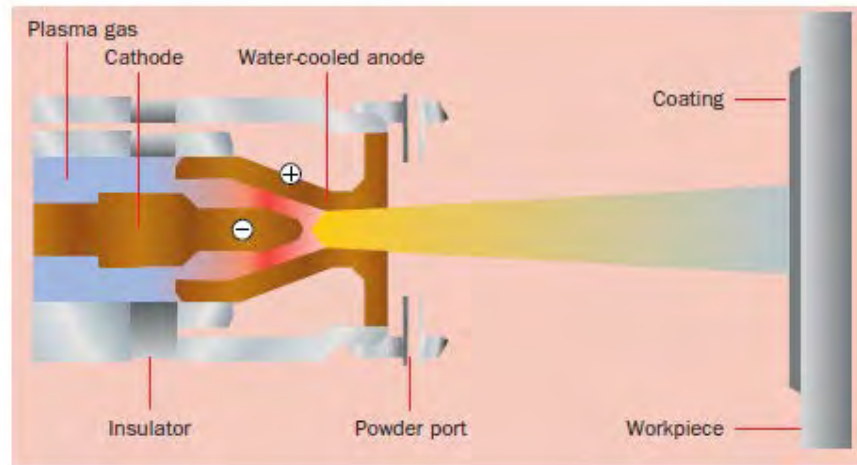
Figure 7.   Plasma spray process, from [20].

C. HEALTH AND ENVIRONMENTAL HAZARDS WITH METAL COATING PROCESSES

Electroplating processes produce toxic gases that not only pollute the environment but impact worker health. Inhalation of toxic emissions, ingestion (e.g., from drinking water), or direct skin contact with plating solutions are typical sources of human exposure to electrolytic CrVI. Moreover, studies [2, 21–23] show that exposure to this hazard heightens human risks of lung cancer, skin lesions, and birth defects. A 2006 final rulemaking identified CrVI as being responsible for 10–45 cases of cancer for every 1000 workers, when compared to six other chemicals, including asbestos and benzene as seen in Figure 8 [2]. Under the same 2006 rule, OSHA proposed a dramatically lower CrVI exposure threshold;

see Figure 9, from 52μg/m^3 to 5μg/m^3 to mitigate health risks [2]. Occupational asthma has also been linked to chrome and nickel electroplating processes [21].

Material	Cancer Risk (per 1000)	Rulemaking Date
Asbestos	6.7	June 1986
Benzene	10	September 1987
Formaldehyde	0.0056 – 2.64	December 1987
Cadmium	3 – 15	September 1992
1,3 – Butadiene	1.3 – 8.1	November 1996
Methylene Chloride	3.6	January 1997
CrVI	10 – 45	February 2006

Figure 8.   Cancer risk of hexavalent chromium (CrVI) in comparison to other known carcinogens, from [2].

Country	Occupational Exposure Limit (μg/m^3)
United States	
• New OSHA (2006)	5
• Previous OSHA	52
European Union, France, Germany, UK, Finland, China, India, Japan	50
Sweden	20
Denmark	5

Figure 9.   Hexavalent chromium (CrVI) occupational exposure limits, from [2].

D.   ALTERNATIVE METAL COATING TECHNIQUES

As previously mentioned, one of the main purposes of industrial metal coating systems is to protect against corrosion. This is especially critical for DOD, which spends billions annually on corrosion maintenance for its systems and infrastructures in Figure 10 [24]. Based on these staggering expenditures, corrosion protection technologies will undoubtedly remain a priority for the sustainability of military operations.

Study year	Data baseline	Study segment	Estimated cost
2007–08	FY2005–06	Navy and Marine Corps aviation	$2.9 billion
	FY2005–06	Coast Guard aviation and vessels	$0.3 billion
2008–09	FY2006–07	Air Force	$4.1 billion
	FY2006–07	Army ground vehicles	$2.0 billion
	FY2006–07	Navy ships	$2.1 billion
	FY2006	DoD—other equipment	$3.1 billion
2009–10	FY2007-08	Marine Corps ground vehicles	$0.3 billion
	FY2007–08	DoD facilities and infrastructure	$2.0 billion
	FY2007–08	Army aviation and missiles	$1.5 billion
2010–11	FY2008–09	Air Force	$5.3 billion
	FY2008–09	Navy and Marine Corps aviation	$2.5 billion
2011–12	FY2008–10	Navy ships	$3.3 billion
	FY2008–10	Army ground vehicles	$1.7 billion
2012–13	FY2009–11	Marine Corps ground vehicles	$0.3 billion
	FY2009–11	DoD facilities and infrastructure	$3.0 billion
	FY2009–11	Army aviation and missiles	$1.9 billion
	FY2009	DoD—other equipment	$3.6 billion
2013–14	FY2009–13	Coast Guard aviation and vessels	$0.3 billion
	FY2010–12	Navy and Marine Corps aviation	$3.7 billion
	FY2010–13	Air Force	$6.0 billion

Figure 10.   Department of Defense cost of corrosion studies, from [24]

DOD's primary mission has been to protect U.S. citizens and its interests; however, it, too, must comply with U.S. Statutes and governing agencies' demand for the limited use of toxic coating materials. Therefore, in 2009, the Under Secretary of Defense issued a memorandum for secretaries of the military departments to limit the use of CrVI in coating systems; exceptional cases would require special approval [25]. Furthermore, the Secretary of Defense directed the following actions be taken to alleviate CrVI impact to operations:

- Invest in appropriate research and development on substitutes.

- Ensure testing and qualification and procedures are funded and conducted to qualify technically and economically suitable substitute materials and processes.

- Approve the use of alternatives where they can perform adequately for the intended application and operating environment. Where CrVI is produced as a byproduct from use of manufacture of other acceptable chromium oxides, explore methods to minimize CrVI production.

11

- Update all relevant technical documents and specifications to authorize use of qualified alternatives and, therefore, minimize the use of materials containing CrVI.

- Document the system-specific CrVI risks and efforts to qualify less toxic alternatives in the Programmatic Environment, Safety, and Occupational Health Evaluation for the system. Analyses should include any cost/schedule risks and life cycle cost comparisons among alternatives. Life cycle comparisons should address material handling and disposal costs and system overhaul cycle times/costs due to any differences in corrosion protection.

- Share knowledge derived from research, development, testing and evaluations (RDT&E) and actual experiences with qualified alternatives.

- Require the Program Executive Office (PEO) or equivalent level, in coordination with the Military Department's Corrosion Control and Prevention Executive (CCPE), to certify there is no acceptable alternative to the use of CrVI on a new system. This requirement also applies to the operation and maintenance of a system during the Operations and Support phase of a system's life cycle.

- For such applications where acceptable alternatives to CrVI do not exist, CrVI may be used. [25]

Some manufacturers have minimized the harmful effects from coating processes by replacing plating anodes—swapping out lead with platinum—altering the plating bath formulation, and instituting better wastewater treatment systems [4]. Unfortunately, these and other measures have led to increasing production costs. As a result, alternative coating techniques that provide the same or similar appearance characteristics, performance properties, and costs have been explored. Some of these advances include the use of trivalent chromium [5, 8, 15, 26–30], nanocrystalline structures of nickel-tungsten [8], high velocity oxyfuel (HVOF) [3], and PVD [3]. Legg et al. [3] posed commercial replacements in Table 1 with performance and costs that rival electrolytic hard chrome processes.

Table 1.   Alternative coating technologies under evaluation, after [3].

Technology	Coating material	Typical component application	Typical purpose	Comments
HVOF	Cr_3C_2/Mo-Ni-Cr	Piston Rings	Wear	OEM only
HVOF	Tribaloy 400, WC-Co	Turbine Shafts, Al bearing surfaces	Fretting, wear, corrosion, hot oxidation	OEM and rebuild
Sputter PVD	CrN, Ti-Al-N, TiN	Hydraulic shafts, molds, pump parts, gears, bearings	Wear, release, erosion, corrosion, decorative	OEM; cannot be thick enough for rebuild. No refinishing needed
Plasma nitride + PVD	CrN, Ti-Al-N	"Soft" steels, hydraulics, molds, shafts, piston rings	Wear, fretting, corrosion, erosion	For relatively soft steel, perhaps Al. No refinishing needed
Arc PVD (thick coating)	CrN, Ti-Al-N	"Soft" steels, hydraulics, shafts	Wear, fretting, corrosion, erosion	For extended wear life, perhaps light rebuild
Laser Cladding	Tribaloy 400, WC-Co	Bearing surfaces, turbine blades, shafts	Wear, fretting, corrosion, erosion	High local temperatures, good metallurgical bond. Must be refinished
Laser CVD	TiN	Bearing surfaces, shafts	OEM, rebuild, wear, fretting	High local temperatures. No refinishing needed.

1.   Trivalent Chromium

Many researchers instinctively targeted trivalent chromium as a viable replacement for CrVI because of its thermodynamic stability and benign qualities. It has been successfully used in decorative chrome plating applications, but has found no commercial success in functional or engineering applications, which require greater thicknesses against abrasion, friction, and wear [4, 29]. Some researchers have shown

that electrodeposition of chromium-carbide (Cr-C) layer with trivalent chromium can result in a thick coating for functional applications; however, this was detrimental to material hardness in some cases [27, 30].

2. Nanocrystalline Structures of Nickel Tungsten

Advances in nanotechnology have affected many sectors of industry, including coating systems. In [8], researchers form the Massachusetts Institute of Technology (MIT) Materials Science and Engineering department explored the use of nanotechnology to achieve a greener alternative to hexavalent chromium. These researchers focused their efforts on the use of nanotechnology in creating a metal with the same desirable properties of CrVI minus the hazards. Furthermore, they created nanocrystalline structures of nickel-tungsten and performed a comparative study with hex chrome to determine that they matched in reflectivity and nickel-tungsten was superior is corrosion resistance. As this stage of development, little is known about the negative impact from human interaction with nanoparticles or the cost necessary to scale this innovation.

3. High Velocity Oxygen Fuel (HVOF)

High velocity oxygen fuel coating is characteristic of a thermal spray coating process, enhancing anti-corrosion and anti-wear properties of the material to which it is applied. Legg et al[3]. researched the technical performance of thick HVOF coatings and determined this coating method to be a suitable alternative to electrolytic hexavalent chrome (EHC) after showing tremendous promise in abusive conditions, processing requirements, and costs. These researchers indicated that HVOF achieves coating thicknesses up to 1 mm, which is very useful in rebuilding worn components.

In 2000, HVOF coating found its way into engineering applications used by DOD. Specifically, Schell et al. [31] collaborated with the Navy, Army, and Air Force Air Logistics Centers to substitute EHC plating on gas turbine engines using thermal spray and HVOF. This strategy was implemented to reduce hazardous waste and lower life-cycle costs over a 3 year trial period. In Figure 11, HVOF was determined to be cheaper than EHC in environmental, coating, pre-treating, and other processing costs for

a coated cylinder [3]. When further compared to EHC, HVOF processing has significantly lower yields in waste [31].
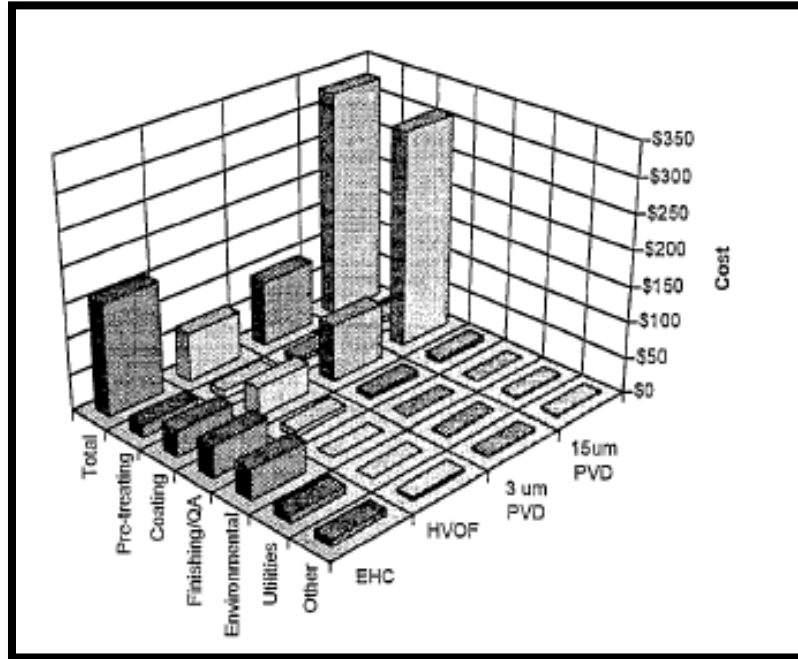
Figure 11.   Cost factor comparison for coating of cylinder with an outside diameter of 125 mm and 300 mm high, from [3]

4.   Physical Vapor Deposition

Physical vapor deposition (PVD) includes thermal evaporation and sputtering methods for the deposition of thin films onto a substrate [17]. As described elsewhere [17], PVD is employed in a number of applications, namely electronic devices, optical and conductive coatings, and surface modifications. When used in decorative applications, 3μm thick PVD processes cost less than EHC; however 15 μm PVD coating is far more costly as shown in Figure 11 [3]. These findings suggest that functional applications of PVD may not be an ideal replacement for EHC.

E.   MILITARY APPLICATIONS OF METAL COATING

Metal coating systems are utilized by essentially every organization across every industry and the military is no exception. The Department of Defense is a large consumer

of this technology. The extensive and expensive inventory of military systems including ships, aircrafts, ground vehicles, weapons, etc., drove the need for standardization of manufacturing processes to ensure delivery of mission capable and mission ready products at a fair price. These measures were aimed at identifying dependable, durable, and maintainable equipment to optimize system performance.

The Department of Defense has long established specifications for chrome and nickel plating to ensure that coated systems meet desired performance criteria prior to installation and subsequent use. Some examples of these of CrVI coated systems are highlighted in Figure 12 [2]. As shown, electrodeposition of hard chrome plating protects against wear but also permits rebuilding of worn parts in aircrafts, vehicles, weapons, hydraulic systems, and landing gear.

Product	CrVI Application/ Process	Purpose	Application	Substrate	Specifications
Anodizing	Chromic Acid Bath	Wear and corrosion resistance, paint adhesion	Aircraft	Aluminum	MIL-A-8625F, Type I, Type IB
Hard Chrome Plating	Electro-deposition	Wear protection, repair/rebuild worn components	Aircraft, vehicles, gun barrels, hydraulic actuators, landing gear		MIL-STD-1501, MIL-C-20218
Chromate Sealant	Incorporated into sealant composition	Water barrier, corrosion inhibitor	Electronics, vehicle panels, fuel tanks, radomes, fasteners, tactical shelters		MIL-PRF-81733, MIL-S-8802
Chromate Primer	Incorporated into primer	Corrosion protection	Aircraft skins, Al airframes, Steel airframes	Aluminum, steel	MIL-F-7179, MIL-P-53022, MIL-PRF-23377, MIL-PRF-85582
Chromate Conversion Coating	Pretreatment bath, wipe, spray	Self-healing coating, sealant for electro-plated and anodized coatings, adhesion surface for paints and sealants	Aircraft skins, Al structures, Mg gearboxes, fasteners, electrical connectors	Al, Mg	MIL-DTL-81706, MIL-C-5541, MIL-M-45202, MIL-A-8625, MIL-C-3171, MIL-C-17711, MIL-M-45202

Figure 12.   Functions and applications of hexavalent chromium in the military, from [2].

16

Electrolytic nickel plating has mostly been replaced with electroless processes. As previously mentioned in [1], electroless nickel plating has seen a successful transition into military applications, particularly aerospace components as seen in Figure 13.

Component	Basis metal	Phosphorus, %*	Coating thickness, mils	Property of interest**
Bearing journals	Al	L, M	1-2	WR, U
Servo valves	Steel	M, H	1	CR, LU, U
Compressor blades	Alloy steels	M, H	1	CR, WR
Hot zone hardware	Alloy steels	M, H	1	WR
Piston heads	Al	M, H	1	WR
Engine shafts	Steel	L, M	1-2	WR, Buildup
Hydraulic actuator splines	Steel	L, M	1	WR
Seal snaps & spacers	Steel	M, H	0.5-1	WR, CR
Landing gear components	Al	M, H	1-2	WR, Buildup
Struts	SS	M, H	1-2	WR, Buildup
Pitot tubes	Brass/SS	M, H	0.5	CR, WR
Gyro components	Steel	L, M	0.5	WR, LU
Engine mounts	Alloy steels	M, H	1	WR, CR
Oil nozzles	Steel	M, H	1	CR, U
Optics	Al	H	3-5	

*Phosphorus content: H = 9 to 12; M = 5 to 8; L = 1 to 2.
**CR = corrosion resistance; WR = wear resistance; U = uniformity; LU = lubricity.

Figure 13.   Aerospace applications of electroless nickel plating, from [1].

F.   REDUCTION EXPANSION SYNTHESIS (RES)

The RES method is a recently developed technique for rapid generation of metal and metal alloy particles, including nanoparticles, from a physical mixture of metal nitrate, oxide or hydroxide species and urea. This mixture is heated in an inert environment at low temperatures (ca. 700°C) [32, 33] and leads to the rapid production of metal and metal alloy particles, primarily on the micron and sub-micron

size scale. The basis of the technology is that metal oxides in the vicinity of volatile reducing radicals and molecules produced by the thermal decomposition of urea, etc., are reduced to metal. The final metal particle size is generally of the scale of the precursor species. Since metal oxide particles of the micron/sub-micron scale are readily produced just by grinding, this is a simple and rapid method for producing micron/sub-micron scale metal. In contrast, the major commercialized techniques employed for making small metal particles, such as "atomization", are limited to particles of order 20 + microns. Although the RES technique has been shown to work very effectively [32,33] in making metal particles much smaller than those available commercially, there is no effort to commercialize at this time.

The fundamental guiding hypothesis of the proposed work is related to the demonstrated RES method. Specifically, it is postulated that if an (metal) object is coated with a typical RES mixture (ca. Cr-nitrate and urea), the RES process (heating in an inert environment) will lead to the generation of a metal surface layer on the object rather than metal particles.

G. MOTIVATION

As mentioned in [24], DOD spends billions annually in corrosion prevention and remediation. This spending is in part due to compliance with regulatory requirements on worker safety and hazardous waste removal associated with electrolytic hexavalent chromium. Costs will continue to climb if proven alternatives are not widely implemented.

Although extensive research has turned up a number of viable replacements to electrolytic coating processes, none has quite matched the totality of effectiveness of EHC needed to trigger a major shift in its usage.

With DOD restrictions placed on the use of hexavalent chromium in various applications due to serious health and environmental risks, it is important to continue to investigate alternatives that will provide the same or better performance capabilities in critical military applications.

18

H. GOALS AND OBJECTIVES

This study is part of a broad effort to find satisfactory nonelectrolytic approaches for producing Cr or Ni coatings on metals. This effort is needed because current technologies are no longer acceptable to DOD as these produce toxic and carcinogenic byproducts. The specific focus of this study was to test the efficacy of a variation on the Reduction Expansion Synthesis (RES) method for creating Cr or Ni coatings on different metal substrates. . RES involves the rapid heating of a metal nitrate and urea mixture in an inert atmosphere to produce pure metal of submicron and nano-size particles [32, 33]. In this study, RES was modified using a number of protocols to "encourage" film growth on specified substrates, rather than particle formation.

THIS PAGE INTENTIONALLY LEFT BLANK

II.   EXPERIMENTAL METHODS

In this chapter the experimental procedures surrounding the generation of metal coatings using variations of the Reduction Expansion Synthesis (RES) method are discussed in detail. These protocols were intended to test non-electrolytic, RES-based, approaches to creating Ni or Cr coatings as both types of metal coating are widely employed, on a number of metals, including stainless steel and magnesium. Due to the novelty of this endeavor, the experiments were tweaked as the study progressed. Specifically, temperature settings, precursor ratios, and even additives were modified to converge on a novel RES based method that would result in the nonelectrolytic deposition of surface layers of Cr or Ni for a variety of metals. The surface cleaning method for the substrates, followed by three variations on particle RES, called Protocols I, II and III, are discussed in detail below.

Each metal included in this investigation was treated with the RES based electro-less Cr and Ni coating. This was followed by characterization of the specimens using optical microscopy, energy dispersive spectroscopy, and X-ray diffractometry to determine the morphology, topography, and composition of the surface layer post-treatment.

A.   SURFACE PRE-TREATMENT OF METAL SUBSTRATES

Various metal wire specimens, ranging from 1–2 inches in length, were used as metal substrates during the experimentation process. The preliminary investigation was carried out with no surface-cleaning of the wires. This served to establish a baseline for future testing. The metal substrates as seen in Figure 14 consisted of the following: 1.15 mm brass wire, 1 mm copper wire, 0.5 mm tungsten wire, 1 mm stainless steel wire, and 0.05 mm nickel wire.
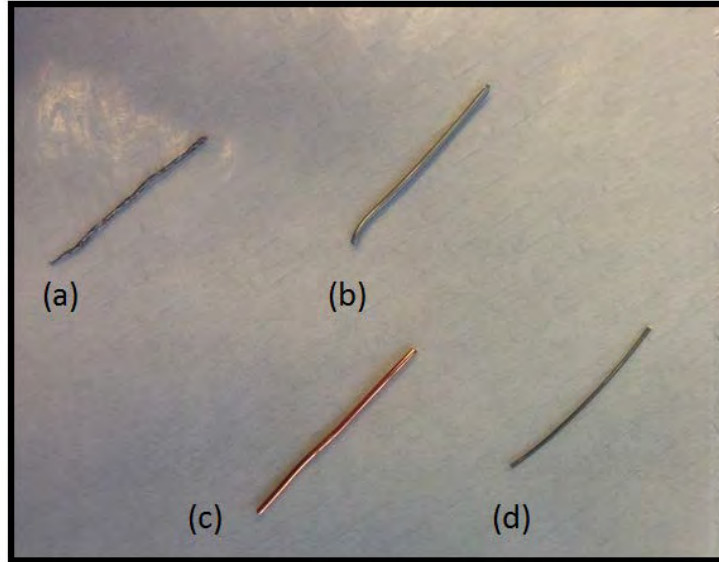
Figure 14.   Metal wires used in the RES-based nonelectrolytic analysis (a) 25–
0.05mm braided nickel wire, (b) stainless steel, (c) copper, and (d)
tungsten. Not shown but also analyzed was brass.

1.   Surface cleaning

Following the baseline experiments, all successive tests were performed on clean
wire samples. Consistent with commercial surface pre-treatment practices, this step was
necessary to promote proper adhesion of the reduced metal from the RES process to the
surface of the substrate. A commercial MAAS metal polish-cleaner was applied to a lint-
free cloth and used to scrub. Next, the substrates were submerged in ethyl alcohol
(ethanol) in a glass beaker. The beaker containing the samples was placed in a water bath
contained in a Branson 2510 ultrasonic cleaner as shown in Figure 15. The ultrasonic
cleaner transferred sound waves to the beaker that attacked the surface of the metals and
in turn removed contaminants form the object. The substrates were immersed in the
ultrasonic cleaner for 3 minutes.

Figure 15.   The substrates were placed in a glass beaker containing ethanol
solvent then cleaned in a Branson 2510 Ultrasonic Cleaner.

B.   RES PROCESS: PROTOCOL I

The RES technique was carried out by physically mixing a metal nitrate with urea in a mortar and pestle until the product appeared visibly homogenous or consistent in color and texture as shown in Figure 16. The ratio of urea to metal nitrate was held constant at 2:1 in these early experiments.
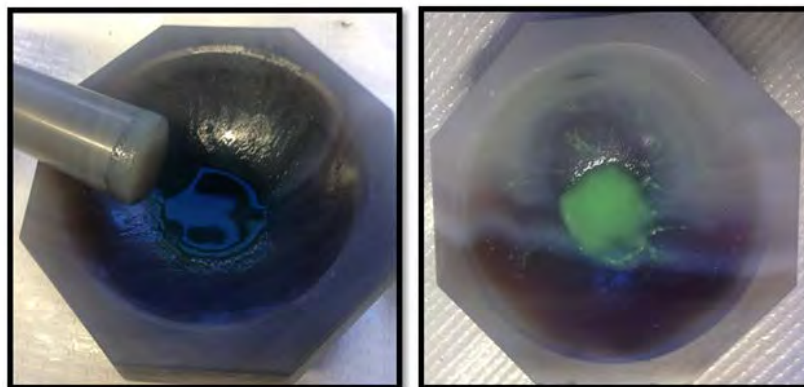
Figure 16.   Physical mixture of Cr-nitrate and urea (left) and Ni-nitrate and urea
mixture (right).

Chromium (III) nitrate nonahydrate (Sigma-Aldrich 99.0 pct) and nickel (II) nitrate hexahydrate (Sigma-Aldrich 97.0 pct) with urea mixtures, in separate experiments, were added to an alumina boat containing brass, copper, stainless steel, tungsten, and nickel substrates. The alumina boat was covered with a second alumina boat then placed in a 20 mm diameter quartz tube. Fittings were attached to both ends of the tube to create a controlled environment. A hose leaving one of the end fittings was connected to a compressed nitrogen gas (N_2) bottle through a Matheson Tri-gas flowmeter. A small hose leaving the other end fitting was positioned underneath a vent hood to collect the exhaust gases. The preloaded quartz tube was placed in a Lindberg Blue M tube furnace such that the alumina boat remained just outside of the furnace enclosure while warming up. N_2 was applied to the tube at a rate of 100 sccm to purge the system of air for about 15 minutes while the furnace was simultaneously being heated to 850°C as illustrated in Figure 17. Portable fans were positioned directly below the end fittings to prevent failure of the o-rings due to elevated temperature conditions.

Figure 17.   RES arrangement with quartz tube positioned in the clamshell
Lindberg Blue M tube furnace and portable cooling fans.

Once the temperature reached 850°C, the gas flow rate was reduced to 10 sccm, and the quartz tube position shifted/pushed until the alumina boat was at the center of the pre-heated furnace. It was repeatedly noted that after this shift of the cold alumina boat to the furnace center, that the furnace temperature dropped by more than 200 degrees. It also was repeatedly noted that within 2 minutes of the shift process, a white byproduct was observed downstream of the flow. Once the temperature stabilized at the set temperature, requiring approximately 5 min, the process proceeded for precisely 3 additional minutes. Once the 3 minutes elapsed, the quartz tube was shifted back to the original position such that the alumina boat was again outside the heated zone. Immediately after this was accomplished the gas flow rate increased to 100 sccm. After 10 minutes the flow of nitrogen gas was halted and the alumina boat was allowed to cool to room temperature. Once cooled, the contents in the alumina boat were collected for analysis.

C.   RES PROCESS: PROTOCOL II

After performing several experiments using a different precursor to urea ratio and constant temperature, the RES process was modified for varied results. First, the temperature was increased to 1000°C to enhance combustion during the synthesis process. Second, a reagent, sodium carbonate monohydrate (Na_2CO_3) (Sigma-Aldrich 99.5 pct), was added to the urea and metal nitrate mixture to remove what appeared to be the formation of excess carbon on the surface using the process described in Section B.

D.   RES PROCESS: PROTOCOL III

Simply combining the modified mixture described in the RES Protocol II was deemed insufficient in promoting a uniform coating on the substrate surface. Therefore, an additional tweak to the experimental conditions was necessary to better achieve the desired results. The major difference between Protocol II and III was the application of the mixture to the substrate. With the introduction of the reagent to mixture as in Protocol II, the mixture became drier and possessed a powder-like quality. In order to make a solution for coating the substrates from this dry powder, approximately 5 ml of ethanol was added to the mixture with a mass ratio of 1:4 (powder:ethanol). Simply dipping the substrates into the wetted powder mix was sufficient to create an adherent layer.

1.   The Dipping Method

The cleaned substrate was dipped in the wet mixture described in Protocol III above then allowed to air dry for approximately 90 seconds. The substrate was then dipped and dried for 2 more cycles. Small amounts of ethanol were added to the mixture during the dipping process to maintain wetness. After the final dip and the substrate dried, it was placed in an empty alumina boat for RES processing.

E.   RES PROCESS: STANDARD PROTOCOL

The purpose of the standard protocol was to determine the impact of temperature on the surface layer of the metal substrate. This step was performed using a clean—polished and ultrasonically bathed—stainless steel wire sample. After cleaning, the wire sample placed in an empty alumina boat, capped with a second boat, then subjected to RES treatment at a temperature of 1000°C. No coating mixture was employed during this process.

F.   CHARACTERIZATION

Material characterization was conducted to determine whether or not the metal nitrate was reduced to pure metal during the synthesis process and whether chromium metal or nickel metal successfully coated the surface of the individual substrates used. The following characterization techniques were used to analyze the resultants of the obtained: optical microscopy, scanning electron microscopy (SEM) with energy dispersion spectroscopy (EDS), and X-ray diffractometry/diffraction (XRD). Each characterization technique provided unique information about the samples and allowed for a comparative analysis pre and post treatment by the RES method.

1.   Sample Preparation

The following preparation processes were important in analyzing the morphology of the samples through the cross sectional arrangement of the treated substrates. Sample preparation for material characterization was carried out in four stages. These stages were sequential and destructive but would prove necessary in collecting a complete analysis of the substrates post-treatment.

a.   Stage 1: Cutting

The treated substrates were cut using a commercial diagonal wire cutting pliers. The substrates were cut to a height that just exceeded the height of the specimen support springs. Cutting the treated wire led to pinching of the cross-sectional surface of the substrate.

b.   Stage 2: Mounting

After the treated substrates were oriented vertically in the holders, they were hot mounted using a commercial conductive filled phenolic mounting compound, KonductoMet. The sample was hot mounted in the hand operated hydraulic Buehler: SimpliMet 2 mounting press as seen in Figure 18. After 10 minutes the heater was removed from around the compound and replaced with a cooling fin. Once cooled, the phenolic pucks seen in Figure 17, were raised from the chamber and prepared for characterization.

Figure 18.   SimpliMet 2 mounting press used for hot mounting the samples in a phenolic puck.

Figure 19.   Phenolic pucks containing RES-treated substrates.

c.   *Stage 3: Grinding*

The phenolic pucks were transferred to the Buehler EcoMet 4 variable speed grinder-polisher with AutoMet 2 power head for grinding shown in Figure 20. The grinding conditions were set to a speed of 150–200 rpm and 4–6 lbs of pressure. A steady water flow was applied during grinding to reduce friction during substrate contact with the grinder. The grinding sequence was performed on 120, 220, 320, 500, 800, 1200, and 2400 sodium carbide grit paper. Due to pinching of the substrate that occurred during cutting, extensive grinding was required in order to produce a smooth cross section for observation in the optical microscope and SEM just below the pinch.

Figure 20.   Buehler EcoMet 4 variable speed grinder-polisher with an AutoMet
2 power head.

d.   *Stage 3 – Polishing*

Polishing of the samples was carried out using an EcoMet 3 variable speed grinder-polisher with an AutoMet 2 power head as seen in Figure 21. Polishing was performed to remove the abrasions caused by grinding. Using the EcoMet 3, the samples were mounted in holder and which was lowered onto a micro-cloth with a pressure of 4–7 lbs. A 1 micron alumina solution was applied to the polishing pad every 3 minutes for 30 minutes. Next a 0.05 micron alumina solution was applied to a separate polishing pad for the same duration as the 1 micron treatment. Polishing with the VibroMet 2 served as an additional step towards achieving a smoother finish. The polishing process using the Vibromet 2 called for the 1 micron and 0.05 micron alumina solution in sequential steps for approximately 2 hours.

Figure 21.   Buehler EcoMet 3 variable speed grinder-polisher with a AutoMet 2
power head (left) and a VibroMet 2 for final finishing (right).

2.   Optical Microscopy

Optical microscopy was performed using a Nikon Epiphot 200 optical microscope as seen in Figure 22. This characterization technique was utilized as an intermediate step between the macroscopic images and the high resolution SEM equipment. The aim was to capture images in the longitudinal and cross-sectional planes at low magnification. To analyze topography in the longitudinal plane, both the pretreated and post-treated samples wires were physically positioned on the stage for comparative analysis. However, the geometry of the substrates resulted in an uncontrollable deflection of the light near the rounded edges, rendering the collection of images an arduous task.
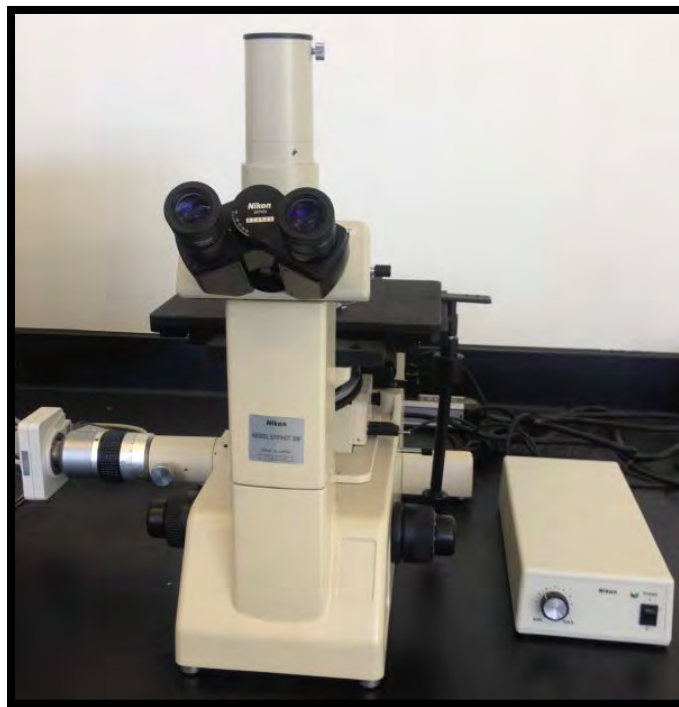
Figure 22.   Nikon Epiphot 200 Optical Microscope.

3.   Scanning Electron Microscopy-Energy Dispersive Spectroscopy

Scanning Electron Microscopy (SEM) was conducted using a Zeiss Neon 40 field emission scanning electron microscope with Energy Dispersive Spectroscopy (EDS) as seen in Figure 23. This characterization technique was carried out to collect micrographs showing the morphology and topography of the substrates pre- and post-treatment. It was necessary to place the samples in a drying oven for approximately 24 hours prior to SEM to ensure no moisture present that would affect its critical components. The instrument parameters during characterization were set to a voltage of 20 kV, a working distance between 6–8 mm, and an aperture size of 60 μm. SEM would assist in determining if a coating was present on the surface of the treated samples. EDS was conducted to determine the elemental characteristics of the treated substrates based on the collected SEM images. EDS provided a quantitative analysis of the surface layer on the substrates that provided chemical composition data as a function of position within the polished wire cross sections. For example, this technique could confirm chrome or nickel deposition, excess carbon, excess oxygen, etc.
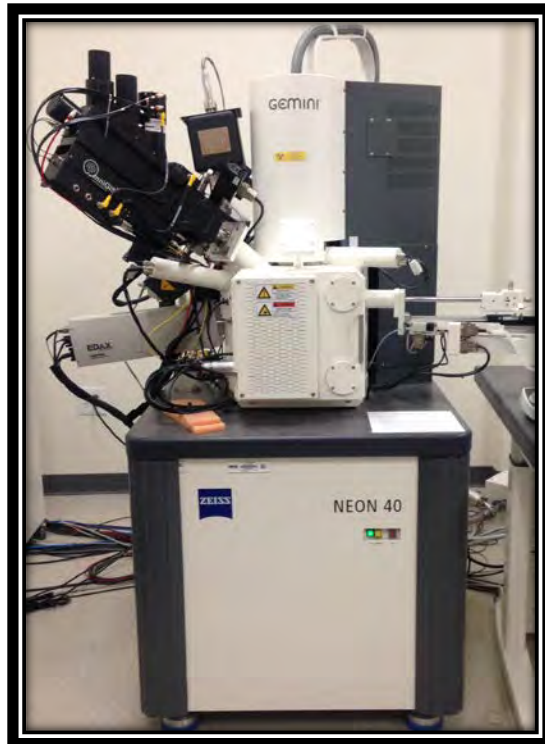
Figure 23.   Zeiss Neon 40 Field Emission Scanning Electron Microscope with
Energy Dispersive Spectroscopy.

4.   X-ray Diffraction

X-ray diffraction was conducted with a Rigaku Miniflex 600 at 40kV and 15mA as shown in Figure 24. The characterization technique was performed to measure the geometrical arrangement of the diffracted X-rays. The intensity versus the 2θ angle was measured over a range from 10–90 degrees. The resulting diffraction patterns were further analyzed using a Rigaku PDXL2 software package to determine the crystallographic structure of the samples. XRD was performed on the powder samples collected from RES Protocol II and III process. This was necessary in order to determine whether the precursors were reduced to pure metal during RES.

Figure 24.   Rigaku MiniFlex 600 used for X-ray diffraction.

THIS PAGE INTENTIONALLY LEFT BLANK

III. RESULTS AND DISCUSSION

The results obtained were based on visual observations and analysis of data collected from the characterization techniques described in Chapter II. The findings varied according to the RES protocol employed, with each modification to the procedures producing different or improved results over previous experiments. In this Chapter the results from the various characterization techniques showing the impact of the precursor-urea ratios, additional reagents, temperature, direct application of the mixture to the substrate metal, and substrate selection are presented and discussed in detail.

A. RES BASELINE EXPERIMENTS

The baseline experiments were carried out using RES Protocol I without cleaning the metal substrates. In these early tests metal substrates were physically surrounded with a paste mixture containing a 2:1 ratio of urea to chromium nitrate, where chromium nitrate served as the precursor. Nickel nitrate was reserved for later experiments. Visual observations obtained following treatment of the substrates are listed in Table 2. Based on initial observations, none of the substrates used in the preliminary experiments appeared shiny in color, consistent with metallic chrome, but instead were covered with a black powdery substance resembling soot. The substrates from the baseline experiments were treated a second time under identical conditions but no noticeable changes in appearance were observed.

Table 2.   RES coating method baseline experiments.

Substrate	Coating Mixture	Visual Observations[1]
Brass	chromium nitrate + urea	III, IV
Stainless Steel	chromium nitrate + urea	II, IV
Tungsten	chromium nitrate + urea	II, IV
Copper	chromium nitrate + urea	I, IV

---

[1] I = Light patches of dark areas on the surface; II = Dark coating on the entire surface; III = Large patches of dark areas on the surface; IV = Black powder particles remained in the alumina boat as byproduct

The small substrates identified in Table 2 were magnified under a light microscope to acquire more qualitative detail of the surface features after baseline treatment. Optical images of the substrates in the longitudinal frame were obtained before and after these early experiments to detect possible changes to the surface topography invisible to the naked eye. Prior to treatment, the unpolished brass metal as seen in Figure 25(a), had a shiny exterior and coarse structure with grooves along the entire surface. After being treated, optical images of the brass substrate highlighted the random dispersion of black particles covering the majority of the exposed areas as shown in Figure 25(b). The stainless steel substrate originally possessed a metallic finish, which was mostly covered with black particles after undergoing the combustion process as seen in Figure 26. The pre-treated tungsten substrate as seen in Figure 27(a), possessed longitudinal markings. After treatment, optical images of the tungsten substrate revealed black powder deposition in Figure 27(b) that was not distributed evenly across the surface. The copper substrate, not shown, had similar characteristics as the other three samples showing deposition of particles on the surface in a random array.
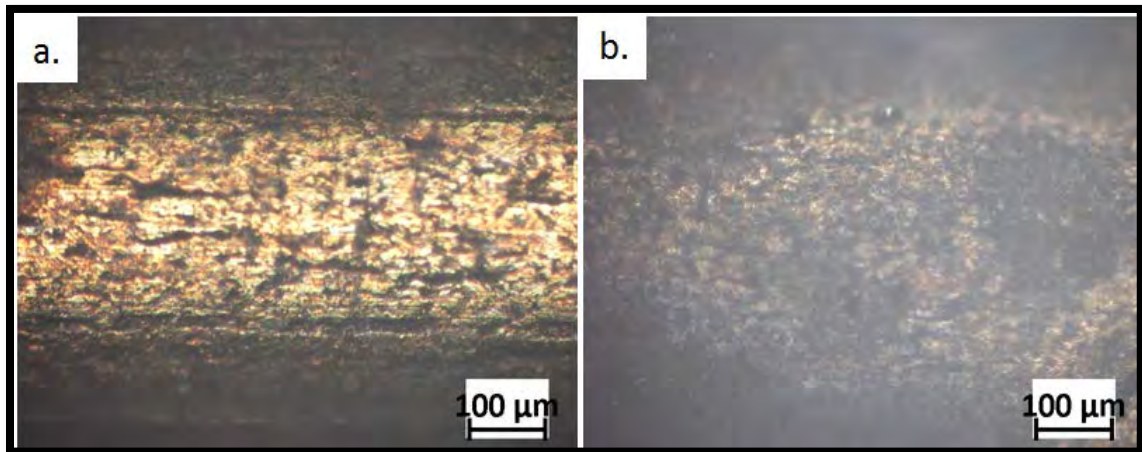
Figure 25.   Optical images of the brass substrate in its longitudinal axis. Image
(a.) is the as-is brass sample without surface preparation. Image (b.)
is brass after the initial attempt to chrome coat. The post treated
sample appears to have a layer of black particles.
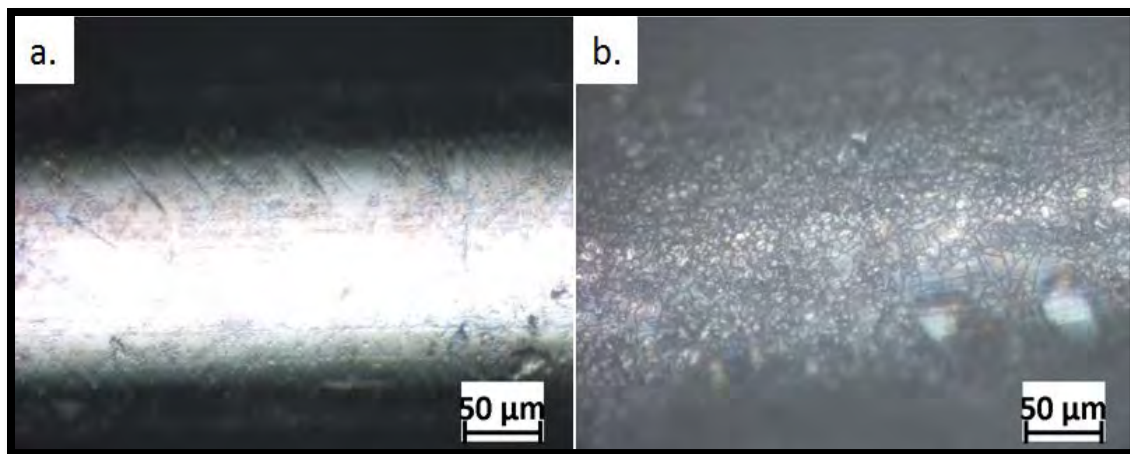
Figure 26.   Side by side comparison of optical images of the stainless steel substrate in the longitudinal plane (a.) untreated sample and (b.) treated sample.
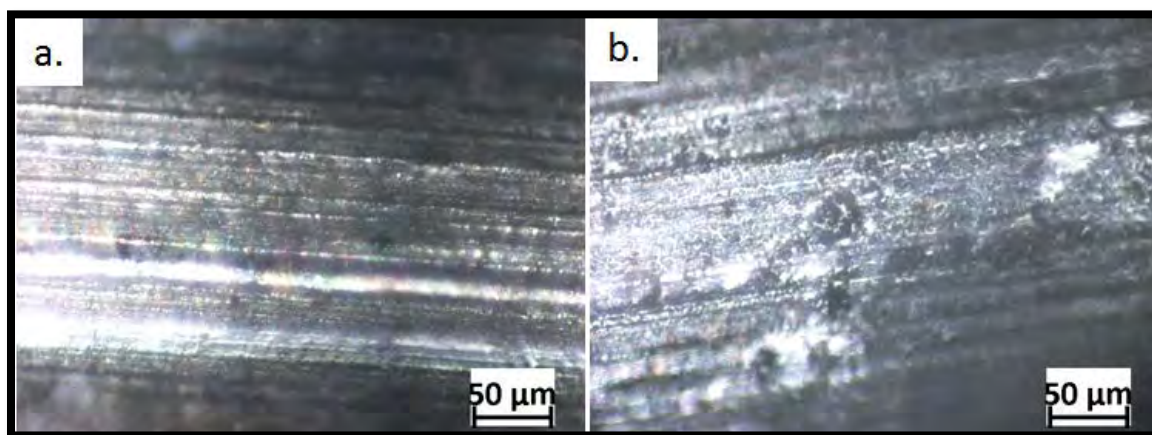
Figure 27.   Optical images of tungsten substrate in the longitudinal plane. (a.) Untreated tungsten metal in (b.) Little evidence of metal on the surface of the tungsten wire.

The baseline experiment in which the brass substrate and the coating mixture were physically combined in the boat produced the dark powder particles shown in Figure 28. These particles were collected and characterized using XRD to determine the identity of the crystalline solid particles. The diffraction pattern seen in Figure 29 was indicative of a phase separation of the chromium nitrate to Carlsbergite ($CrN_{0.95}$) or chromium nitride, during thermal decomposition of the physical mixture. There was no evidence showing a breakdown of the brass surface layer having a direct interaction with the resulting powder.

Figure 28.   Black powder particles remaining in the alumina boat following treatment of the brass substrate.
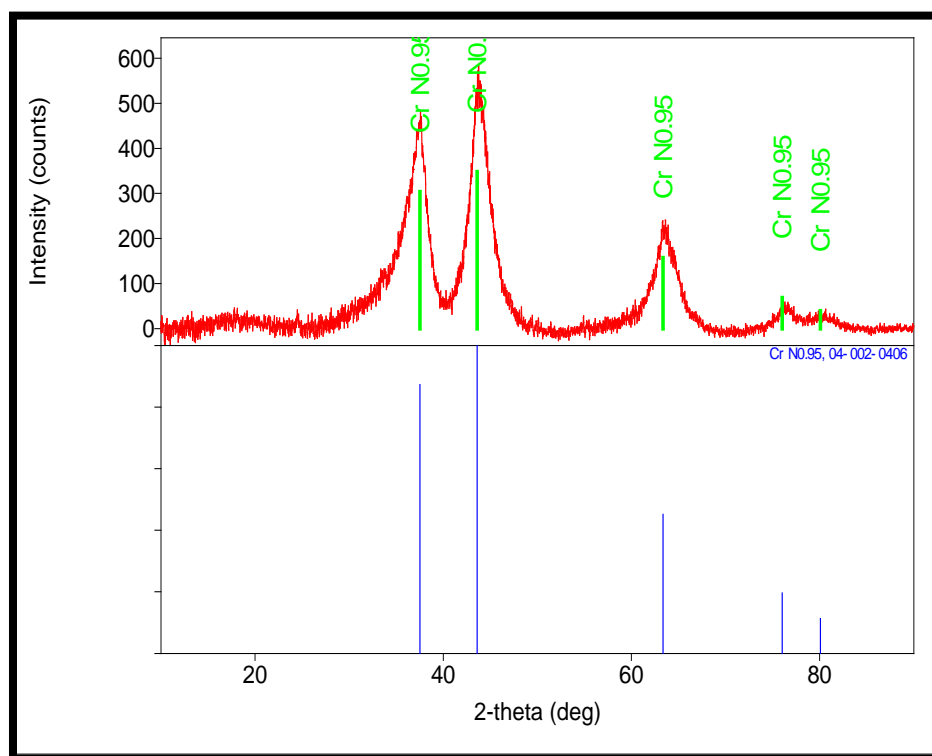
Figure 29.   XRD of the black powder particles recovered from the alumina boat used in the brass experiment. The powder was determined to be chromium nitride ($CrN_{0.95}$).

The tungsten and stainless steel wires were combined in the same boat with the coating mixture during the experiment. Consistent with the brass substrate the powder particles analyzed were also determined to be chromium nitride having a 1:1 solubility of

38

chromium to nitrogen in Figure 30. The XRD pattern corresponding to the copper substrate listed in Table 2 was also consistent in classifying the residual particles as chromium nitride. Bai et al. [34] produced chromium oxide from the thermal decomposition of Cr-urea mixture heated to 300°C in air for 2 hours. The major difference between both analyses is the environmental condition during treatment. In the case of the RES process, after urea fully decomposed under the high temperatures, the gases produced were pushed downstream under the steady nitrogen gas flow and nitrogen deposited on the remaining chromium metal to form chromium nitride.
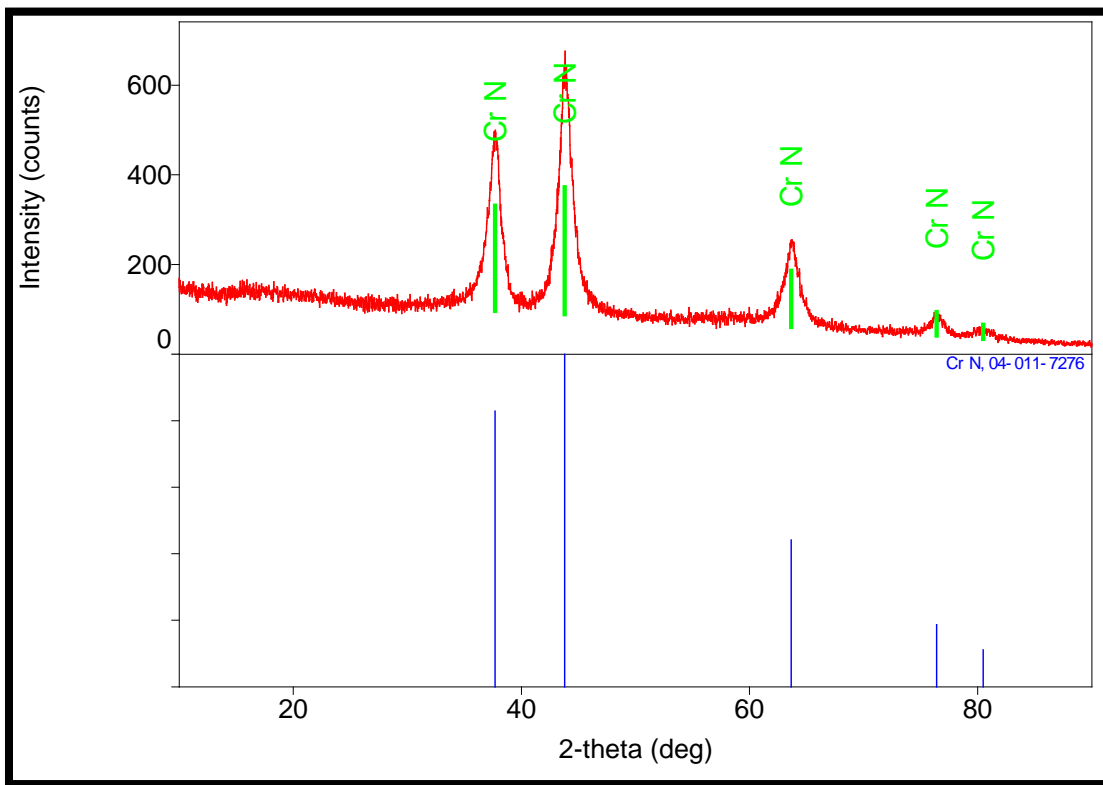
Figure 30.   XRD pattern for the powder particles produced during the treatment of stainless steel and tungsten in the RES baseline experiment.

B.   RES PROTOCOLS

To limit the amount of carbon produced in the surface coating and oxidation, various modifications to the baseline experiments were employed. As in all commercial coating processes, it is critical to ensure the surface of the metal being coating is properly

prepared through aggressive cleaning in order to produce strong bonds with the coating metals. Once the surfaces were prepared as described in the Chapter II, a number of experiments were performed varying the parameters of different substrates to converge on successful chrome or nickel coatings.

Initial experiments using RES Protocol I produced a surface with high carbon content as seen in the baseline experiments. This was verified using EDS characterization. A noticeable reduction in the carbon levels on the surface was observed after evaluating samples from RES Protocol II, but oxygen was unintentionally introduced in higher quantities as a result. The intention of RES Protocol III was to bring the metal released by the reducing inherent in RES in direct contact with the surface. Thus, the metal could coat the surface, but not require any volatile metal containing species to form. As noted, it is clear from the results of Protocol I, particularly the formation of metal containing particles in the alumina boat, that the metal is not volatile at any stage. It remains close to its original location. Thus, for the metal to collect on the wire surface it must initially be on the wire surface. Coating the wire with a metal containing precursor mix appears the best method for meeting this requirement.

Table 3 contains various samples treated under the indicated experimental conditions. Some of the results highlighted are further discussed in detail according to the RES method employed. The majority of the samples collected from the various RES experiments were further analyzed using one or more of the characterization techniques described in Chapter II of this study. A summary of the results from applying these RES protocols on 26 metal substrates are captured in Table 4. Samples that did not undergo further analysis due to being deemed unsuccessful, were not the subject of further probing.

Table 3.   Sample preparation methods based on RES protocols employed.

Sample No.	Protocol[2]	Substrate[3]	Coating Mixture[4]	Comments[5]
1	I	SS	C1	1:2
2	I	SS	C1	1:5
3	I	W	C1	1:2
4	I	Br	N1	1:2
5	I	Cu	C1	1:2
6	II	W	N2	1:2:4, 1000°C
7	II	SS	N2	1:2:4, 1000°C
8	III	W	N2	1:2:4
9	III	Cu	C2	1:2:4
10	III	Cu	N2	1:2:4
11	III	SS	N2	1:2:4
12	III	Ni	C2	1:2:4
13	III	Br	C2	1:2:3
14	III	Ni	C2	1:2:3
15	III	SS	C2	1:2:3
16	III	W	C2	1:2:4
17	-	SS	none	Control, 1000°C
18	III	Cu	C2	1:2:1, 850°C
19	III	W	C2	1:2:1, 850°C
20	III	SS	C2	1:2:1, 850°C
21	III	Cu	C2	1:3:1
22	III	W	C2	1:3:1
23	III	SS	C2	1:3:1
24	III	SS	C2	1:2:1
25	III	SS	C2	1:2:2
26	III	SS	C2	1:2:3

[2] I = Surface pretreated with metal polish and rinsing with ethanol in an ultrasonic bath. No Na_2CO_3. Physical mixing in mortar and pestle. Mix and substrate physically combined in alumina boat only to 850° C for 5 min; II = Surface pretreated with repeated metal polishing and rinsing with ethanol. No Na_2CO_3. Physical mixing in mortar and pestle. Mix then added to substrate boat. Heated to 850° C for 3 min;

III = Surface treatment with repeated metal polishing and rinsing with ethanol. A mix containing urea:metal nitrate:Na_2CO_3 wetted with ethanol. Wetted mix painted on substrate, dried, and repeated 3X. Heated to 1000° C for 3 min.

[3] SS = Stainless steel wire with a 1.0 mm diameter, 77% AT Fe, 18% AT Cr, and 5% Ni; Cu = Pure copper wire with a 1.0 mm diameter; W = Pure tungsten wire with a 0.5 mm diameter; Br = Brass wire with a 1.15 mm diameter; Ni = pure nickel wire with a 0.05 mm diameter

[4] C1 = Physical mixture with the ratio of chromium nitrate:urea; C2 = Physical mixture of the ration of chromium nitrate:urea:Na_2CO_3; N1 = Physical mixture of the ratio of nickel nitrate:urea; N2 = Physical mixture of the ratio of nickel nitrate:urea:Na_2CO_3

[5] Ratios of the compounds in the coating mixture and temperature settings inconsistent with normal treatment for specified RES protocol process

Table 4.　Summary of Results

Sample No.	Analysis Method[6]	Coating Thickness[7]	Comments[8]
1	a, b	5 µm	3, 4
2	a, b, c	5 µm	1, 5
3	a	-	-
4	e	-	analysis on powder only
5	visual only	-	-
6	e	-	analysis on powder only
7	e	-	analysis on powder only
8	a, b, c	-	2
9	a, b, c, d	-	2
10	a	-	-
11	a, b, c, d	16 µm	4, 6
12	a, b, c	-	1, 4
13	visual only	-	-
14	a	-	-
15	a, b, c, d	15 µm (O), 10 µm (I)	1, 3, 6
16	a	-	-
17	a, b, c	-	-
18	a, b, c	-	1, 3
19	a, b, c	-	2, 3, 5
20	a, b, c	10 µm	1, 4
21	a, b, c	-	1, 5
22	a, b, c	-	2, 5
23	a, b, c	12 µm (O), <1 µm (I)	2, 5
24	a, b, c	8 µm (O), 8 µm (I)	1, 4
25	a, b, c	11 µm (O), 5 µm (I)	1
26	a, b, c	8 µm (O), 5 µm (I)	1, 5

---

[6] a = Optical microscope; b = SEM; c = EDS spot analysis; d = EDS mapping; e = XRD

[7] O = outer surface layer; I = Inner surface layer

[8] 1 = Metal oxide ratio in coating > 4/1 suggesting little oxidation; 2 = Metal Oxide ratio in coating < 4/1 suggesting high oxidation; 3 = Clear indication of Cr enrichment in surface layer; 4 = Carbon < 10%, similar to bulk; 5 = Carbon > 10% in the surface layer; 6 = Porous appearance in surface layer;

C.   RES PROTOCOL I

Samples 1–5, as indicated in Table 3, were treated using Protocol I (850°C for 5 minutes). Samples 1–4 were treated with Cr-nitrate precursor:urea coating mixture, while Sample 5 was treated with Ni-nitrate precursor:urea coating mixture. Similar to the baseline experiments, the metal substrates were either completely covered in black powder or displayed a random dispersion of black particles on the surface after treatment. The stainless steel samples (Samples 1 and 2); however, revealed the formation of a surface layer, not observed in the bulk material. This was indicative of a possible successful coating on the surface, was further analyzed. The tungsten substrate (Sample 3) revealed no distinct change in morphology. The brass substrate (Sample 4) showed little sign of powder deposition on the surface and received no additional characterization. Powder particles of the copper substrate (Sample 5) were analyzed to determine crystalline structure.

1.   Optical Microscopy

Optical images of Sample 1 (SS 850°C w/1:2 mix) and Sample 2 (SS 850°C w/1:5 mix) revealed the formation of a surface layer in both cases, having similar appearances. The average thickness in both samples measured 5 μm (Figure 31).
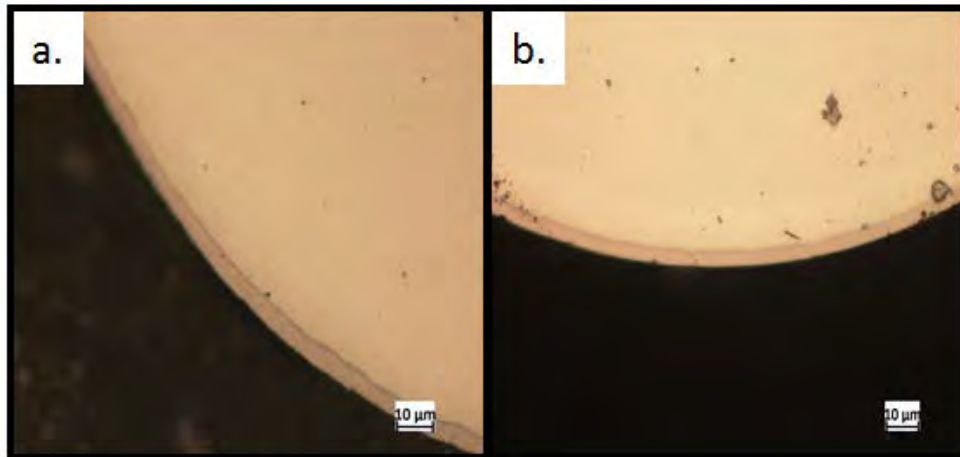
Figure 31.   (a) Surface layer formed on Sample 1 (SS @ 850°C w/1:2 mix) and (b.) surface layer formed on Sample 2 (SS @ 850°C w/1:5 mix).

Optical image for Sample 3 (W @ 850°C w/1:2 mix) as shown in Figure 32, revealed no distinct outer layer on the perimeter of the substrate. As a result of a perceived unsuccessful coating, Sample 3 (W @ 850°C w/1:2 mix) was not subjected to further characterization.
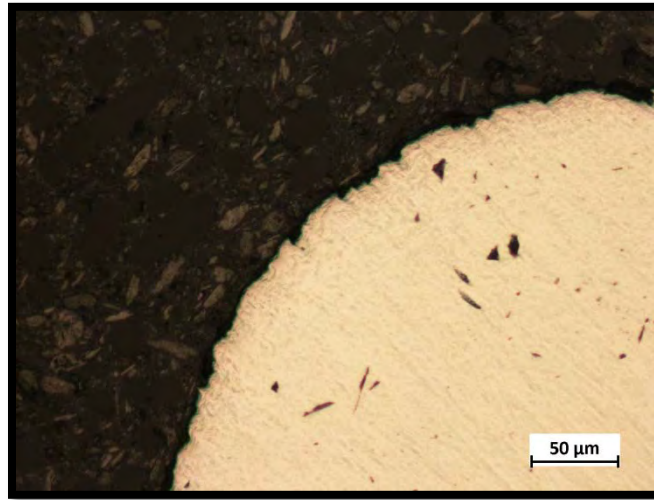
Figure 32.   Optical image of the tungsten wire in Sample 3 showed no distinct surface coating.

2.   SEM

SEM micrograph was obtained for Sample 1 (SS @ 850°C w/1:2 mix) confirming the presence of the surface layer observed from optical imaging. The layer as seen in Figure 33, presents a more detailed structure of the surface deposition. The coating formed was observed as being relatively uniform in size and distribution and even slightly raised from the flat surface.
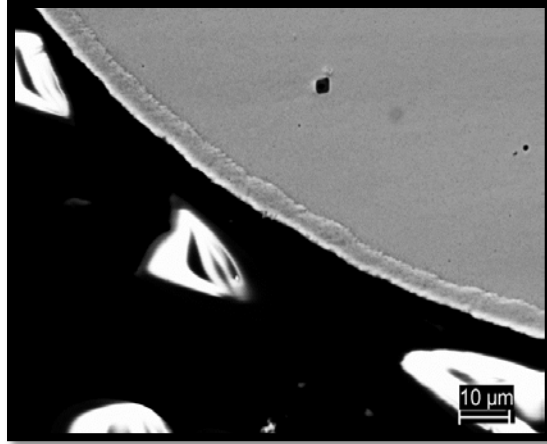
Figure 33.   SEM micrograph of Sample 1 (SS @ 850°C w/1:2 mix) highlights a
topcoat that was formed during the combustion synthesis process.

3.   EDS

The SEM micrograph was collected in the EDS software to investigate the elemental composition across the selected region. In Sample 1 (SS @ 850°C w/1:2 mix) EDS spot analysis of the surface layer showed a strong signal of iron in the substrate compared to chromium, which was lower in the surface layer (Figure 34). This migration of the iron from the surface and deposition of chromium was indicative of chromium enrichment. There was also evidence of little oxidation in Sample 1. The resulting EDS spectrum and quantitative analysis of Sample 2 (SS @ 850°C w/1:5 mix) are shown in Figure 35. The analysis indicated impurities on the surface including nitrogen and oxygen that can be attributed to the decomposition of urea. The metal to oxygen ratio in the spot analysis was 6, suggesting little oxidation. However, the carbon content was 21 at%, more than twice the composition in the bulk material.
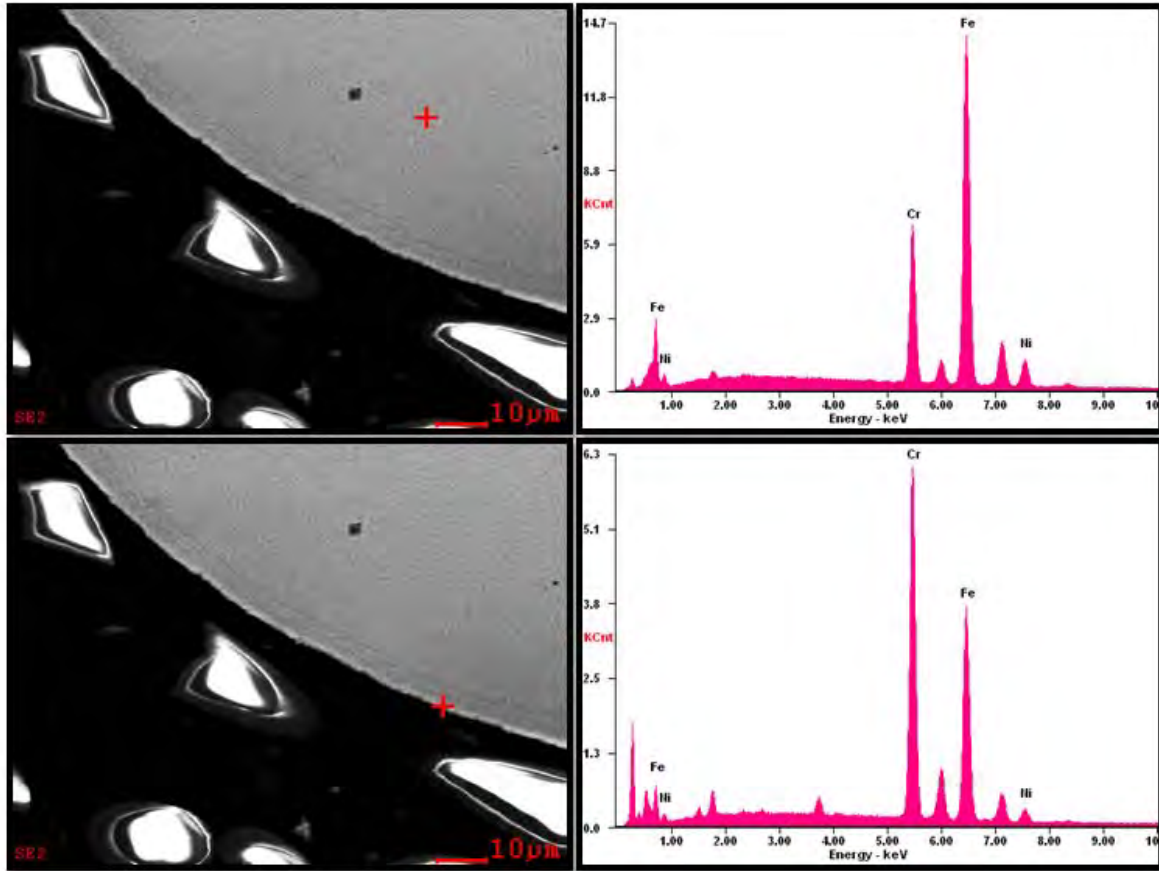
Figure 34.   EDS spot analysis of substrate (top) and surface layer (bottom) in Sample 1 (SS @ 850°C w/1:2 mix).

Element	At%
CK	20.92
NK	07.49
OK	10.40
CrK	10.93
FeK	39.56
NiK	10.70
Matrix	ZAF
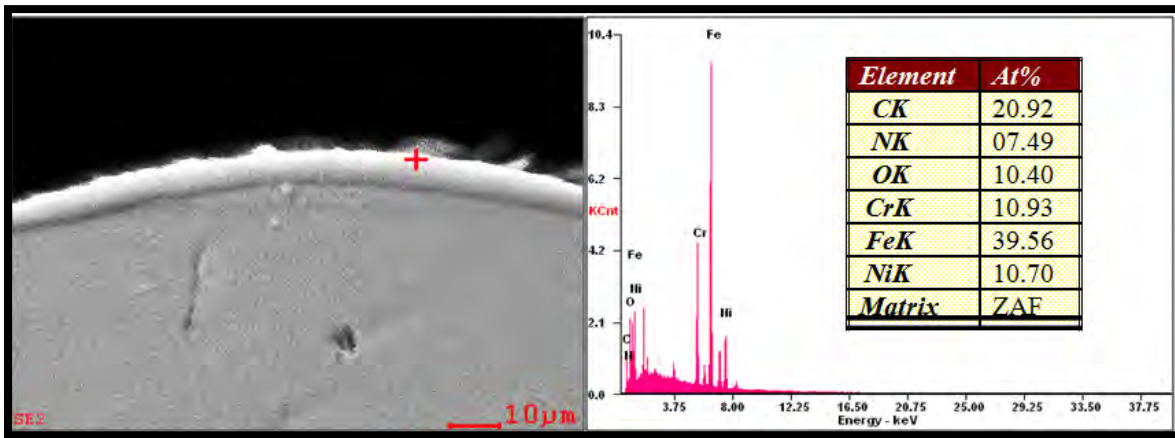
Figure 35.   EDS analysis of the surface layer in Sample 2 (SS @ 850°C w/1:5 mix).

4. XRD

The powder particles generated from Sample 5 (Cu @ 850°C w/1:2 mix) as seen in Figure 36 showed a crystalline structure consisting of Ni metal, Ni oxides, and Ni nitrates.
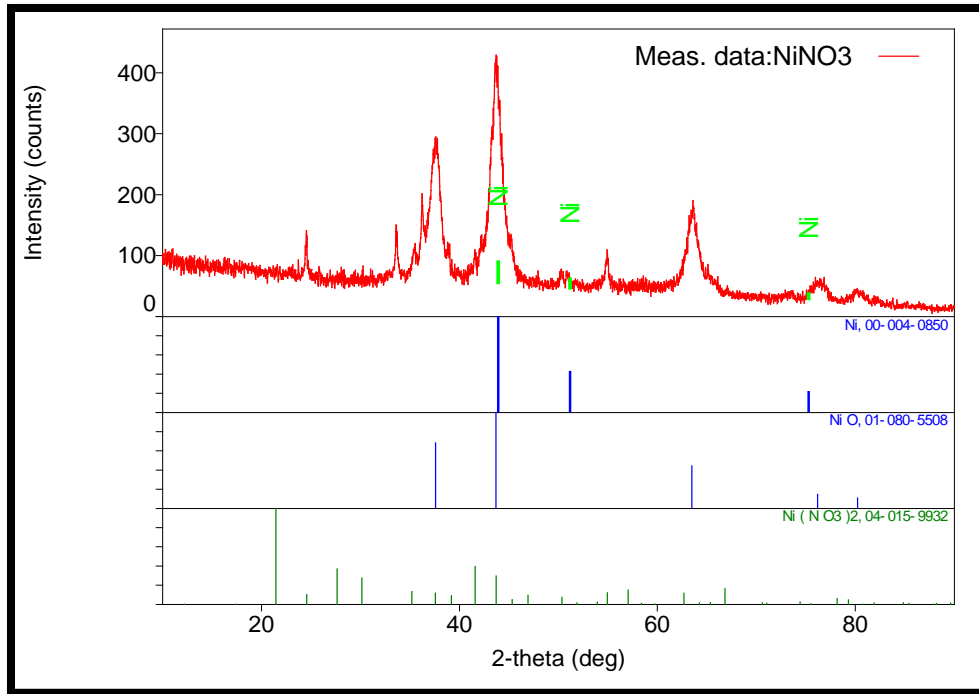
Figure 36.   XRD of powder collected from Sample 4 (Br @ 850°C w/1:2 mix).

D.   RES PROTOCOL II

Protocol II was employed to remove impurities in the surface layer deposited during Protocol I. Sample 6 (tungsten) and Sample 7 (stainless steel) were treated using a coating mixture containing a 1:2:4 ratio of nickel nitrate:urea:Na_2CO_3, respectively. These experiments were performed at 1000°C for 3 minutes. Na_2CO_3 was added to help burn-off carbon.

The notion that sodium carbonate solid could help burn carbon stemmed from the use of this material as a coal combustion catalyst. As demonstrated by Gow and Phillips [35] as well as Mims et al. [36] and Mims and Pabst [37-38] coal combustion particles of

carbonate are found directly on the coal surface. Upon heating, oxygen in the carbonate interacts with the underlying coal to produce carbon oxides. The sodium carbonate is regarded as a catalyst, rather than a reactive reagent, because oxygen in the gas phase regenerates the carbonate, and the cycle repeats over and over.

The temperatures employed in coal combustion are generally greater than 800°C, hence it was reasonable to postulate under the conditions employed herein, that the carbonate could essentially act in the same fashion. That is, the oxygen in the carbonate can be expected to form volatile carbon oxides with the carbon in the surface layer created by the RES process. However, in the RES process the carbonate must be regarded as a reagent. There will be no "reforming" of the original material once oxygen is lost to the carbon combustion process. In coal combustion, carbonates are added at approximately the 1 wt% level because the material is a catalyst. In the RES process, the loading of carbonate must be far greater. There must be enough oxygen in the original loading to burn off excess carbon. Clearly, a potential caveat is that oxygen may not only react with carbon. Possibly the oxygen in the carbonate can oxidize metal as well, or even preferentially. This suggests that an overload of carbonate could have detrimental results. A second caveat is the ultimate disposition of any sodium after the carbonate loses all its excess oxygen.

Prior to treatment, the physical mixture of the nickel nitrate, urea, and Na_2CO_3 appeared as dry and light green powder particles. Following treatment, the metal substrates were found to be covered in clumps of white and dark gray flakes that were attached to the samples (Figure 37). The byproduct formed from the mixture and substrate added directly to the boat for RES was collected from the boat. Visual observations were white and gray powdered particles. XRD analysis was performed on the byproduct to determine phase identification. As seen in Figure 38, the composition of the powder contained Na_2CO_3, suggesting either reduction of that additive did not take place or that the carbonate reformed upon exposure to air. The presence of pure nickel metal indicated a reduction of the nickel nitrate during combustion. This reduction to pure metal has been proven by Luhrs et al. [32] by use of the RES process.

48
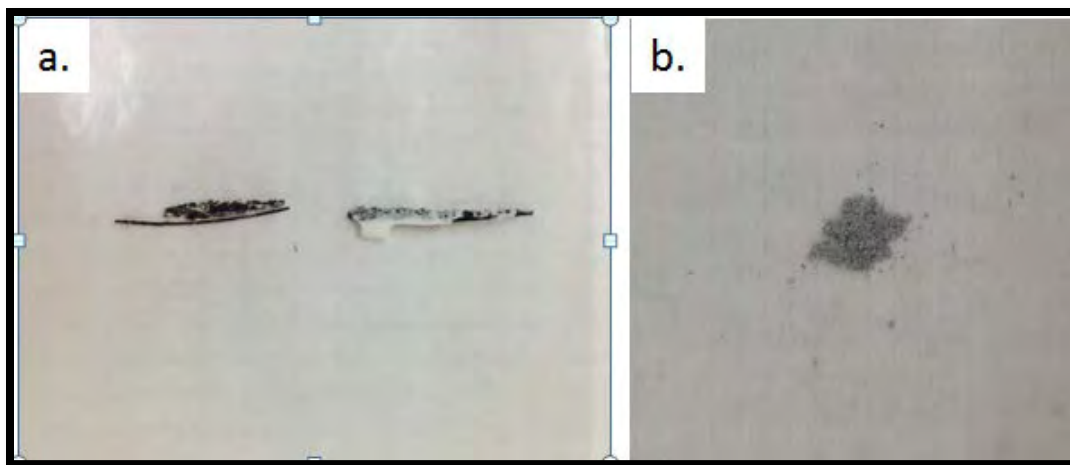
Figure 37.   (a.) Clumps of mixture attached to Sample 6 (tungsten) (left) and
Sample 7 (stainless steel) (right) after treatment. (b.) The byproduct
collected in the boat contained gray powder particles.
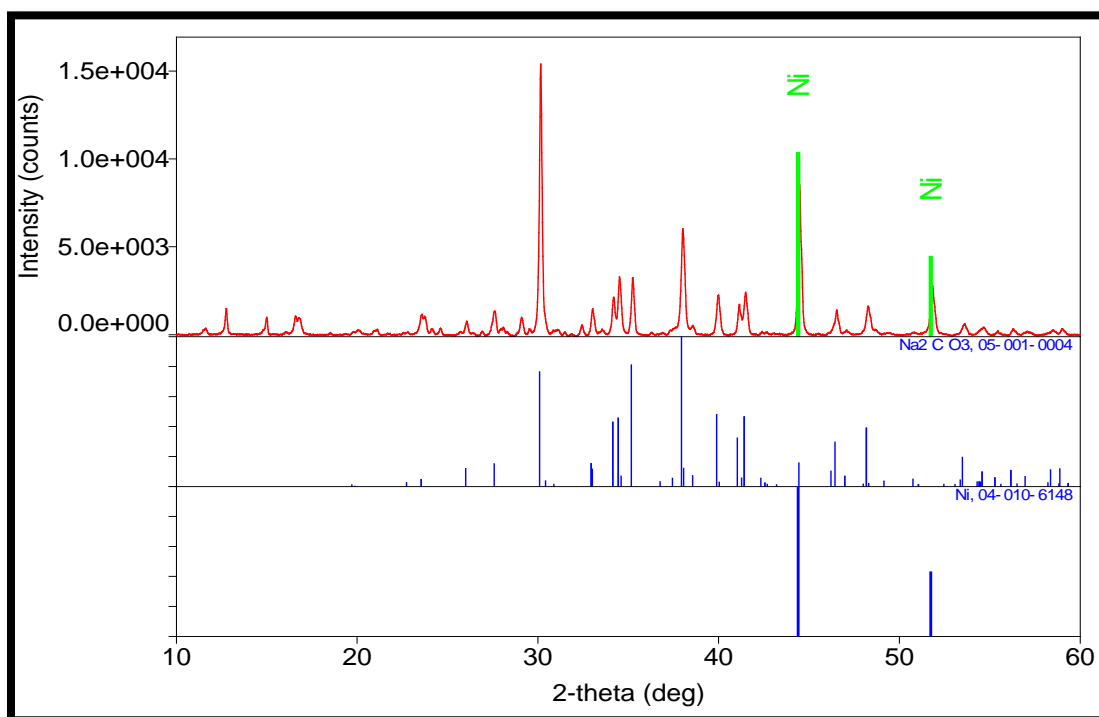
Figure 38.   XRD pattern of the powder particles collected from the alumina boat
after treatment using Protocol II.

E. RES PROTOCOL III

The clumps of Na_2CO_3 attached to the surface of Sample 6 (tungsten) and Sample 7 (stainless steel) were indicative of excess reagent added to the coating mixture. As a result, Protocol III was a 2-in-1 modification RES coating process by adding ethanol to the physical mix and changing the application of the coating mix to the substrate with a dipping method. The remaining samples underwent Protocol III with some variations to the experimental conditions, namely the precursor employed, the temperature, and the mixture ratios.

1. Nickel Nitrate Experiments

Sample 8 (tungsten), Sample 9 (stainless steel), and Sample 10 (copper) were dipped in a homogenous mixture of nickel nitrate, urea and Na_2CO_3 at a 1:2:4 ratio then heated to 1000°C for 3 minutes. Following RES-treatment, these samples were characterized using one or more of the following analytical techniques: optical microscopy, SEM, EDS spot analysis, and EDS mapping. Consistent with the chromium nitrate experiments, no powder particles were produced during this Protocol.

a. Optical Microscopy

Optical images were collected for each of the samples. When Sample 9 (stainless steel) was placed under the light microscope (Figure 39(a.)), a similar surface layer observed on the stainless steel substrates employed in experiments using chromium nitrate as the precursor was seen. Unlike those samples however, only one layer formed along the outer edge of Sample 9 (stainless steel) and the texture of the coating appeared coarse. A discontinuous layer was observed on the perimeter of Sample 8 (tungsten) as seen in Figure 39(b.), suggesting partial coating success. Magnification of Sample 10 (copper) at 20X—higher magnifications were out of focus due to light diffraction—did not reveal alteration of the sample topography (Figure 439 (c.)). As a result, Sample 10 (copper) was determined to be unsuccessful and was not exposed to advanced characterization.
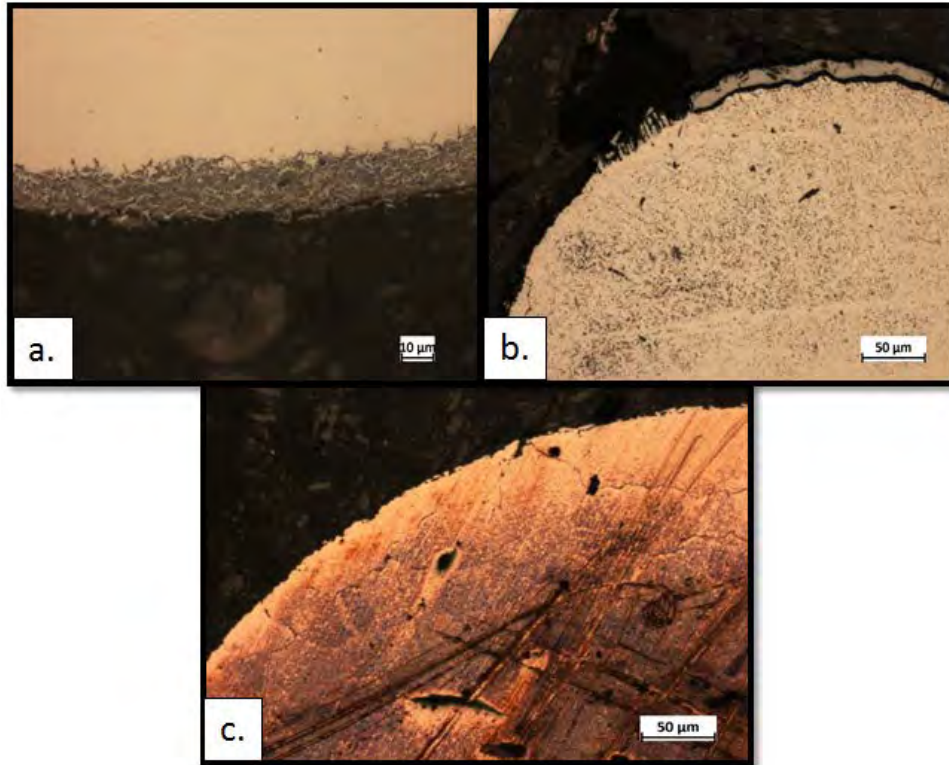
Figure 39.   Optical images of (a.) A distinct surface layer on Sample 9 (stainless steel). (b.) Sample 8 (tungsten) appeared to have a partial coating that was discontinuous along the edge. (c.) Sample 10 (copper) showed no distinct surface layer.

b.   SEM

Sample 9 (stainless steel) was characterized using SEM as seen in Figure 40. The backscattered detection imaging revealed a porous morphology in surface coating formed during treatment with the nickel nitrate-containing mixture. The secondary electron micrograph obtained showed the formation of a solid inner layer not previously observed as well as a bright outer region resulting from the emission of electrons from the edge.
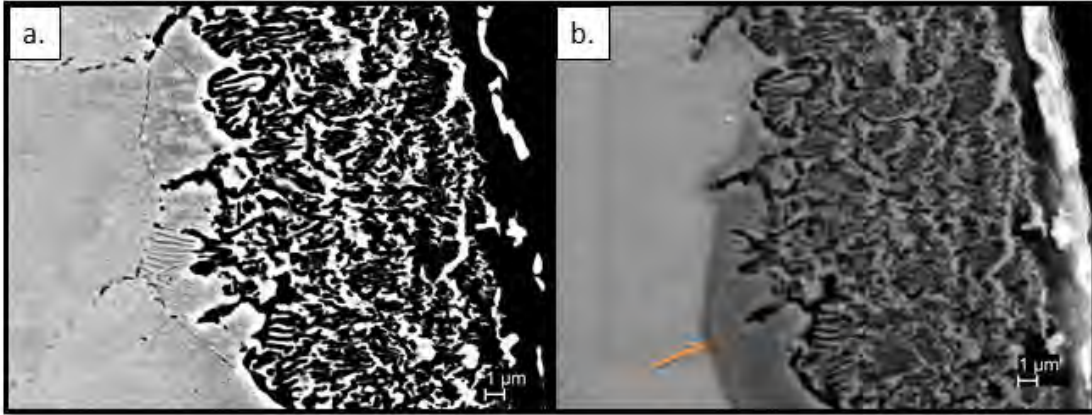
Figure 40.   SEM micrographs of Sample 9 (stainless steel). (a.) Backscattered detection imaging showed a porous appearance in the coating formed. (b.) Secondary electron imaging presented a solid inner layer indicated by the orange arrow.

Sample 8 was also characterized using SEM as shown in Figure 41. Consistent with optical imagery, the coating mixture did not adhere to the surface during treatment. The separations and cracking seen throughout the mixture supports the findings from this and previous protocols that suggest the surface properties of tungsten prevented cohesive bonding of the coating mix to the bulk material.
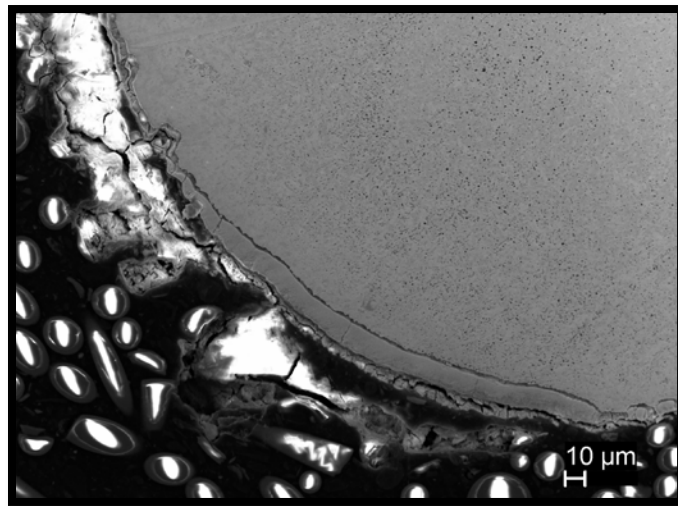
Figure 41.   SEM micrograph revealed disorganized clumps of coating mixture around the outer surface showing little fusion between the mixture and the treated substrate.

52

c.   EDS analysis

EDS spot analysis and mapping of a selected region on Sample 9 (stainless steel) following treatment revealed negligible change, <2 at%, in the nickel content (Figure 42). Chromium was unexpectedly enriched in the sample compared to the bulk stainless steel metal as indicated by the stronger peaks observed. The surface was noticeably oxidized during treatment. Carbon content also increased suggesting deposition during as the urea decomposed under elevated temperatures. Leftover sodium from the reagent was also deposited on the surface.
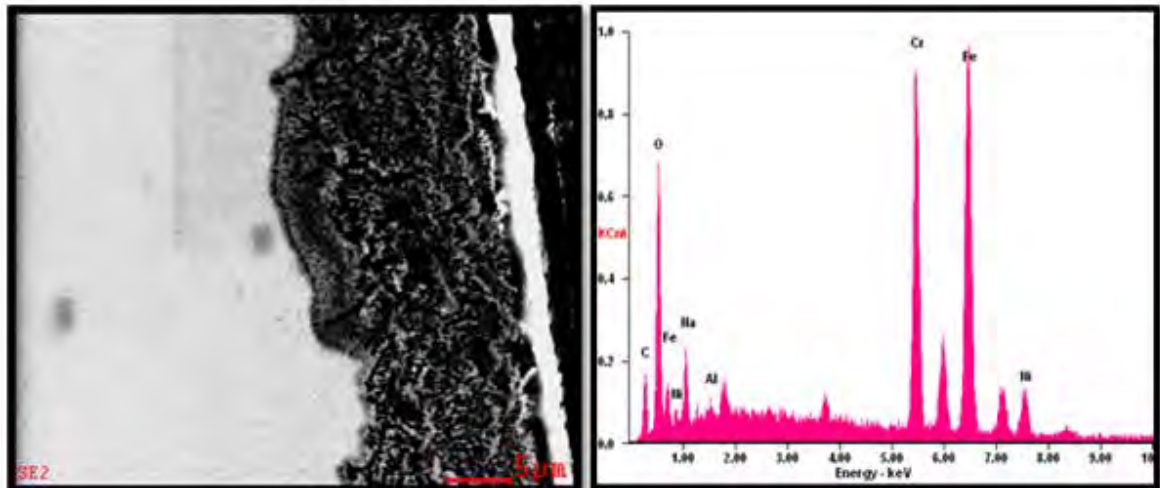
Figure 42.   EDS mapping of the target area (left) on Sample 9 (stainless steel).

Sample 8 (tungsten) was further analyzed using EDS spectroscopy. The distribution of elements present at a targeted spot inside the clumps of coating mixture surrounding the metal is shown in Figure 43. Tiny traces of reduced nickel were identified along with considerable amounts of oxygen.
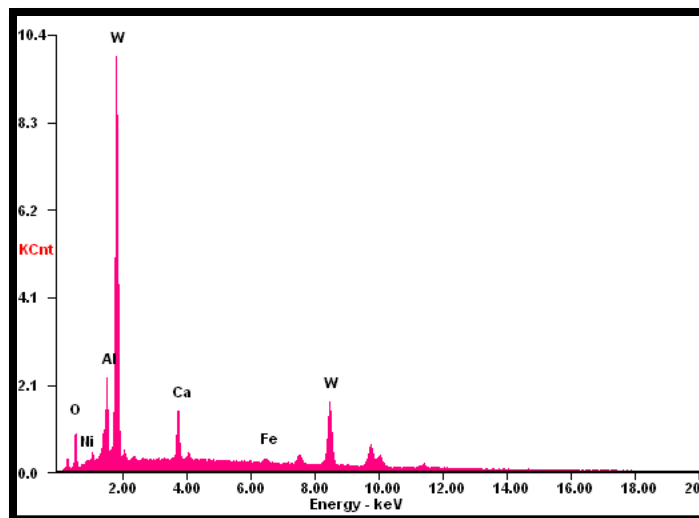
Figure 43.   EDS spot analysis on the outer edge of Sample 8 (tungsten) showed
a weak nickel peak and the presence of oxygen on the surface.

2.   Chromium Nitrate Precursor

Sample 12 (stainless steel), Sample 16 (tungsten), Sample 11 (copper), and Sample 14 (nickel) were treated with a coating mixture of 1:2:4 ratio of chromium nitrate:urea:Na_2CO_3 to 1000°C for 3 minutes. Sample 15 (stainless steel) was treated under the same conditions as the other samples except for being dipped in coating mix having a ratio of 1:2:3. All of the aforementioned samples were first subjected to optical microscopy to magnify the macroscopic features observed. Sample 13 (brass) only did not undergo characterization beyond visual observations due to limited metal deposition on the surface during treatment. No powder particles were produced during this RES process.

a.   *Optical Microscopy*

Optical microscopy revealed a thin discontinuous dark layer was observed around the outer edges of Sample 12 (nickel) and Sample 11 (copper) as seen in Figure 44(a.) and (b.). This prompted the use of advanced characterization techniques using SEM and EDS software to gather more details on the coating formed. Two adjacent surface layers were discovered in Sample 15 (stainless steel) via the light microscope. The inner layer on Sample 15 (stainless steel) measured 9 μm and the outer layer was 11 μm in thickness.

54

Consistent with the previous protocols, the tungsten substrate used in Sample 16 showed no evidence of a topcoat using this protocol or previous protocols and as a result was not subjected to additional characterization.
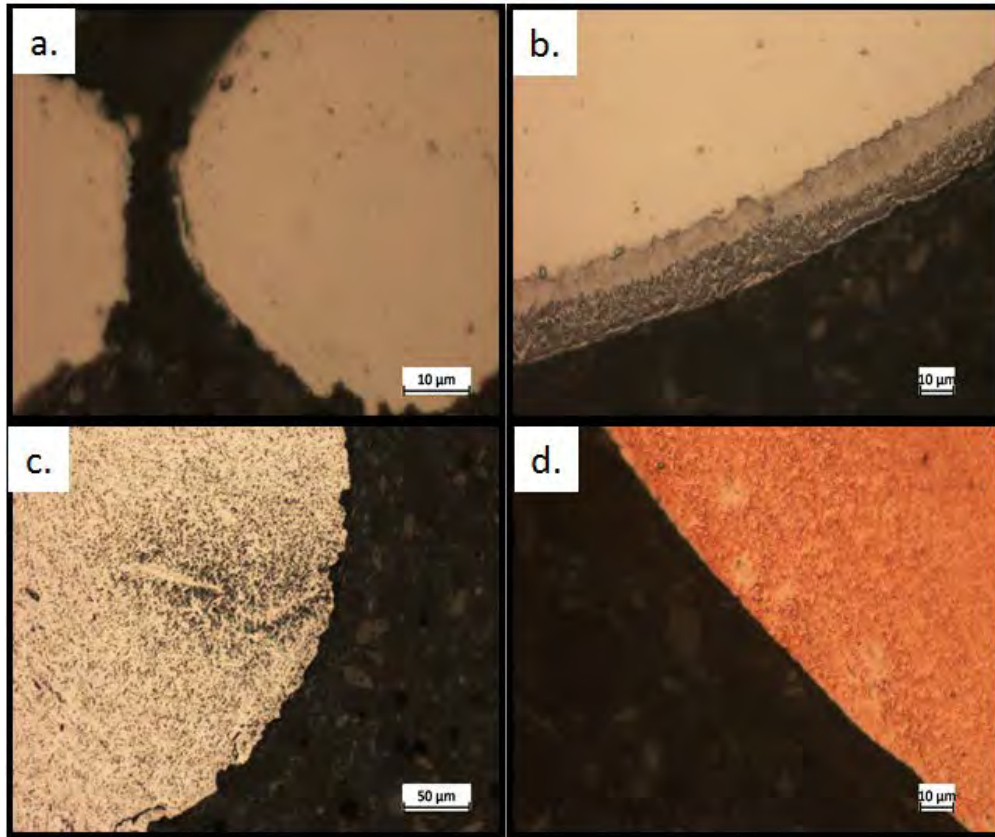
Figure 44.   Optical images of (a.) Sample 12 (nickel), (b.) Sample 15 (stainless steel), (c) Sample 16 (tungsten), and (d) Sample 11 (copper).

b.   SEM

SEM micrographs of Sample 12 (nickel), Sample 15 (stainless steel), and Sample 11 (copper) provided more detail of the focused outer region in ascertaining whether or not Protocol III was successful in producing chromium coating on the treated samples. The appearance of Sample 12 (nickel) as seen in Figure 45(a.) as viewed through the electron microscope did not show any structural changes in the material. Instead, the micrograph displayed brighter edges along the metal surface due to secondary electrons imaging. Characterization of Sample 15 (stainless steel) in Figure 45(b.) revealed 2

distinct morphological changes on the outer edge of the substrate. The inner layer contained small elongated pits throughout. The outer layer was very porous in appearance containing features similar to the inner region coupled with larger pockets in an organized arrangement. The SEM image of Sample 11 (copper) shown in Figure 45(c.) presented incomplete fusion of the coating mix to the surface, with areas of branchlike cracking. It is interesting to note that standard "hard chrome" coatings produced using electrodeposition methods contain a multitude of "micro cracks".
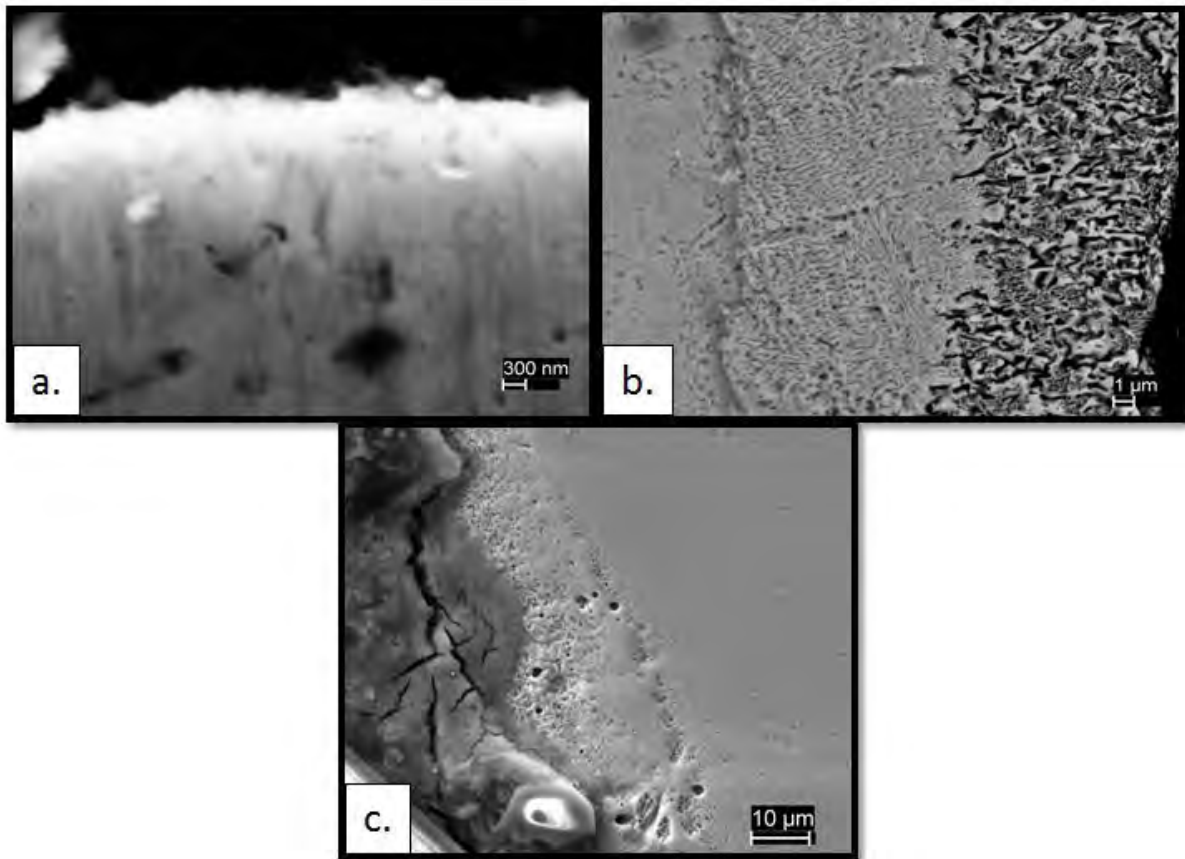
Figure 45. SEM micrograph of Sample 12 (a.) revealed no distinct coating on the edges. In Sample 15 (b.) two distinct changes in morphology was observed after treatment. Sample 11 (c.) showed a partial adhesion of the coating mixture to the surface.

c.   EDS Analysis

Elemental analysis of Sample 12 (nickel) (Figure 46) revealed < 6 AT% deposition of chromium on the nickel surface. However, this metal deposition was not uniform since weak chromium peaks were also detected in the substrate. When compared to the bulk material, the treated sample contained <10 AT% oxygen on the edge suggesting little oxidation during the process. Furthermore, the elemental composition of the surface contained more than 30 AT% carbon. This is consistent with the light microscope observation of a dark thin layer. The carbon was deposited on the surface during decomposition of the urea.
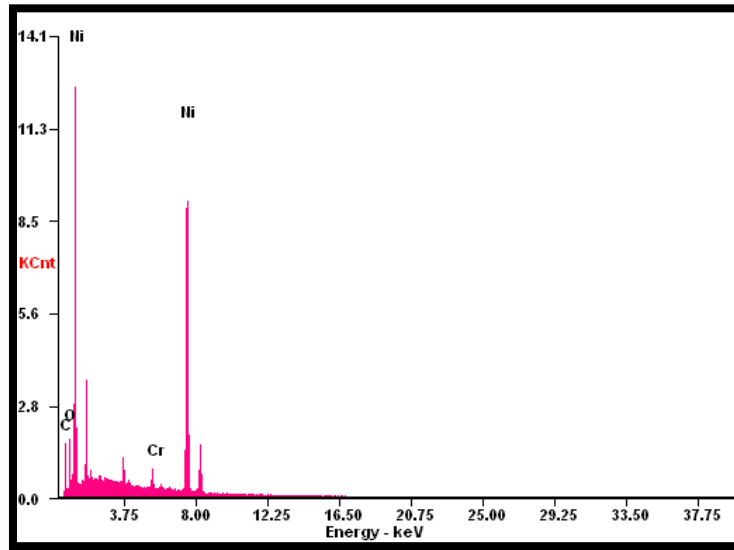
Figure 46.   EDS analysis of the outer region of Sample 12 showing mostly
nickel metal, with traces of chromium, <10 AT% oxygen and a
strong presence of carbon deposited during the breakdown of urea.

EDS spot analysis of Sample 15 (stainless steel) targeted the surface layers identified in the characterization techniques previously discussed. A quantitative profile on targeted areas of the scanned SEM image is shown in Figure 45(b.). When compared to the bulk material in Figure 47(a.), the inner layer formed as seen in Figure 47(b.) displayed constant levels of carbon, a slight increase in the metal-oxide ratio now at 4 AT%, and chromium enrichment on the surface. The results also indicated low carbon

57

content, < 5 AT%, on the outer layer as seen in Figure 47(c.), a metal-oxide ratio > 5/1 suggesting little oxidation, and small amounts of sodium. EDS mapping of the selected region confirmed that this Protocol process introduced oxygen on the surface as well as traces of sodium on the outer edge as seen in Figure 47(d.).
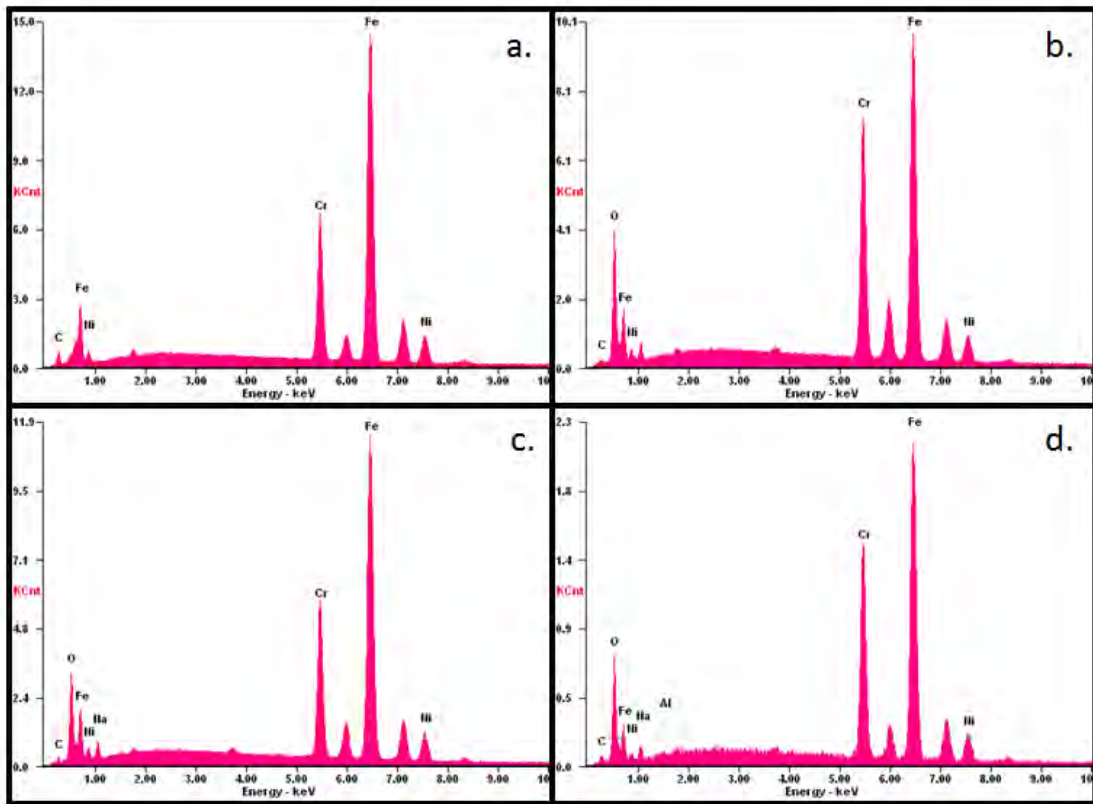
Figure 47.   EDS analysis of Sample 15 (stainless steel) (a.) Elemental composition of the bulk material. (b.) Inner layer formed (c.) The outer layer formed (d.) The EDS map of the scanned region.

Sample 11 (copper) underwent EDS analysis including, spot selection and mapping across the scanned region. EDS mapping (Figure 48) summarized the elemental composition of the target area, which not only confirmed the presence of oxygen and carbon, not normally found in pure copper, but also highlighted the occurrence of chromium on the surface. The chromium layer formed supports the ability of the RES process to deposit metal on a surface, however, the process would require refinement in order to reduce the impurities (carbon and oxygen) and create a uniform coating.
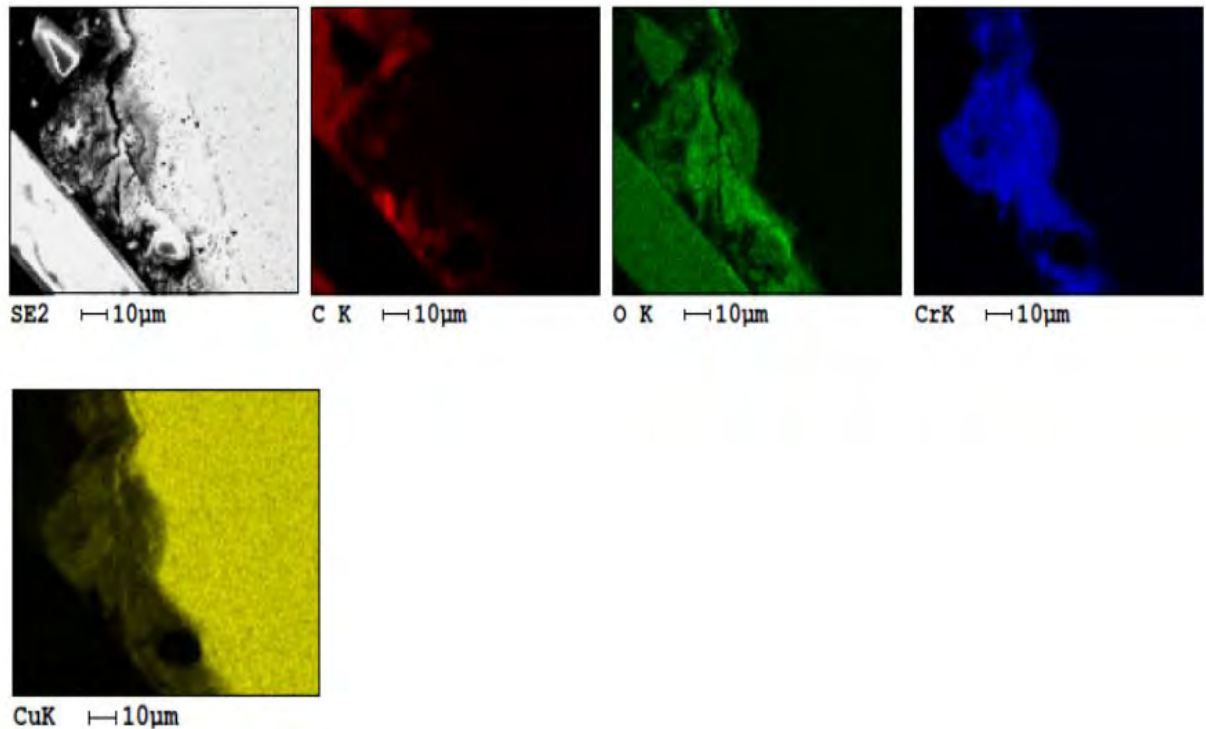
Figure 48.   EDS mapping of Sample 11 (copper) revealed carbon (C), oxygen (O), chromium (Cr), and copper (Cu) in the scanned region.

F.   HEATING ONLY PROTOCOL

A control study was conducted of the stainless steel metal substrates to determine if a surface layer could be produced simply by heating. Specifically, a typical stainless steel substrate was treated using Protocol I method, which is the standard heating protocol, which ends with a 3 minute soak at 1000°C in a flow of nitrogen gas. The substrate so treated was compared to a bulk stainless steel wire that was polished and cleaned to determine the impact of temperature on the surface properties and appearance of the substrate. Visual observations, as seen in Figure 49, revealed a color change from shiny metallic to dark gray after being subjected to a heat treatment at 1000°C in a nitrogen environment.
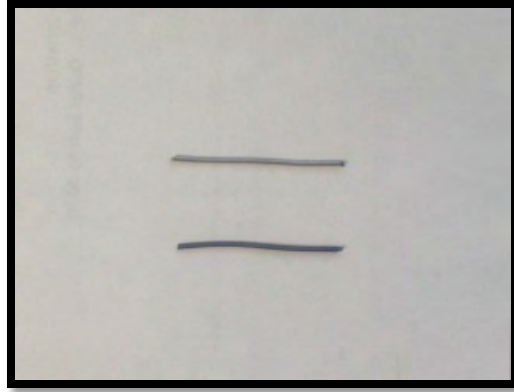
Figure 49.   Visual comparison of the bulk stainless steel (top) and the controlled
sample (bottom).

Optical images (Figure 50) revealed minimal impact to the sample topography as a result of the temperature gradient. A slight dark tint was observed around the edges of the heat treated sample, but no other contrasts in the surface features were observed under the light microscope. SEM images however, revealed a thin film along the contour of the heat treated sample compared not seen in the bulk material at higher magnifications as seen in Figure 51.
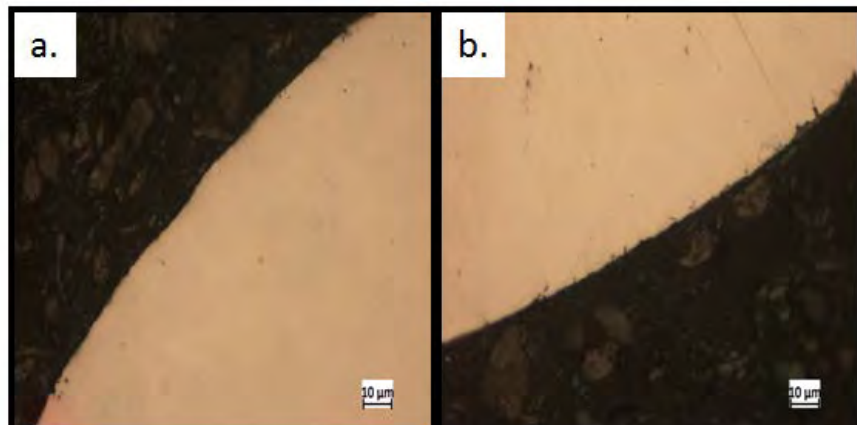
Figure 50.   Optical images of stainless steel sample (a) clean stainless steel
sample and (b) clean and heat treated stainless steel sample. No
significant change to the morphology was observed.
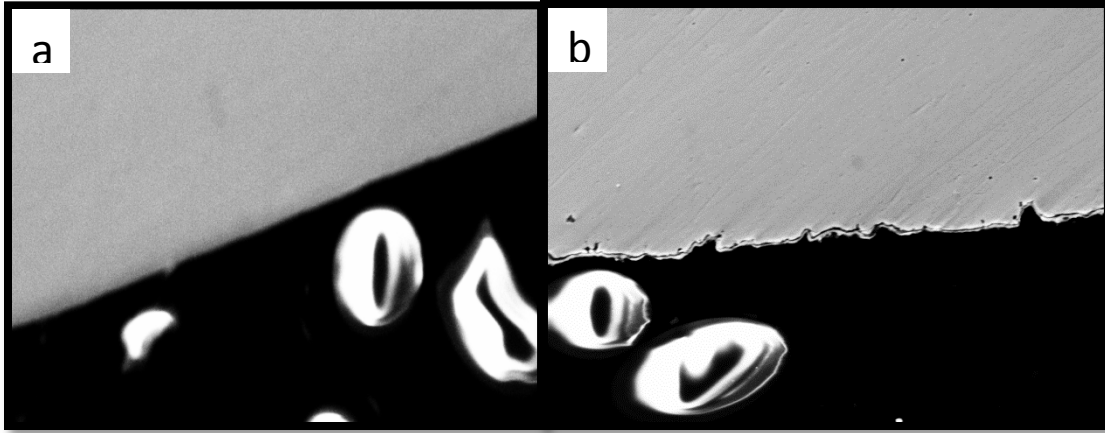
Figure 51.   SEM micrographs of stainless steel samples at 1kX magnification.
(a.) cleaned sample (b.) cleaned and heated 1000°C.

The EDS elemental analysis (Figure 52) of the original stainless steel sample had a composition given in weight percent of 70Fe-18Cr-9Ni-3C. As evidenced by EDS, the heat treated sample showed presence of oxidation on the thin layer formed during treatment (Figure 53). Since the standard protocol was performed in an inert environment, one possible explanation for the oxygen intrusion is a breach in the experimental set-up.
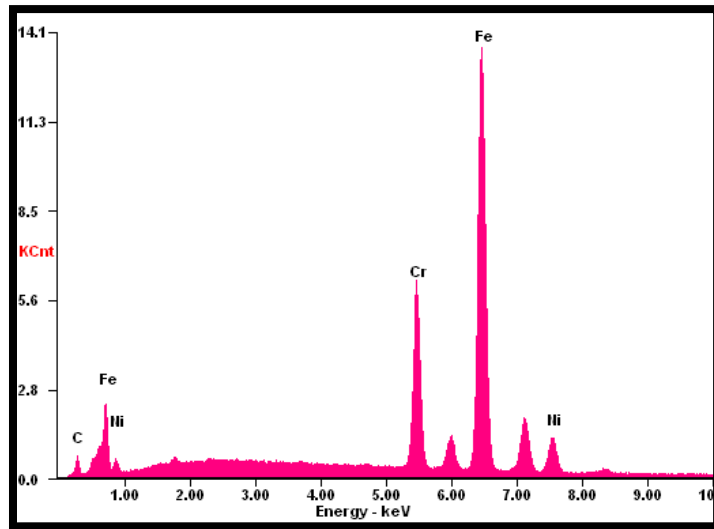
Figure 52.   EDS analysis of the outermost edge of the clean stainless steel wire
only, showed low carbon content in the substrate, which is typical in
the bulk material.
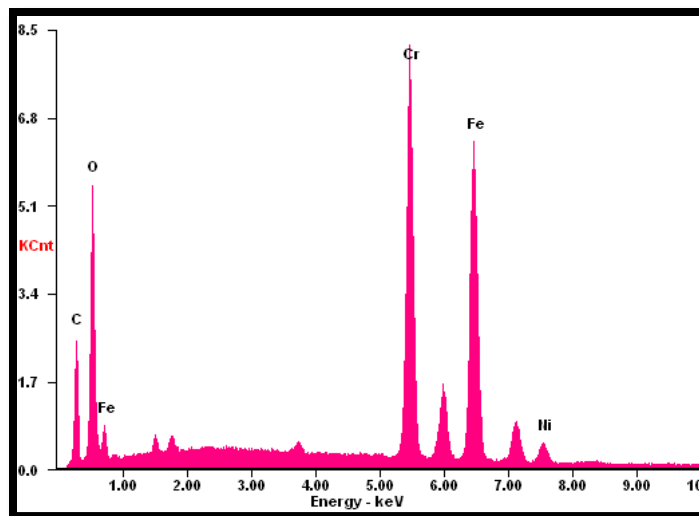
Figure 53.   EDS analysis of the heat treated stainless steel wire showed some oxidation and carbon enrichment in the surface layer.

G.   EFFECT OF TEMPERATURE AND UREA RATIO CHANGES

Sample 18 (copper), Sample 19 (tungsten) and Sample 20 (stainless steel) from Table 3 were treated with Protocol III at 850°C at a 1:2:1 ratio of Cr-nitrate:urea:Na_2CO_3. Sample 21 (copper), Sample 22 (tungsten), and Sample 23 (stainless steel) also underwent RES Protocol III but at 1000°C and a 1:3:1 ratio of Cr-nitrate:urea:Na_2CO_3. A comparative analysis of the copper, tungsten, and stainless steel samples was performed to determine the impact of these variables on the resulting surface characteristics.

1.   Comparison of Copper Substrate

The copper substrates, Samples 18 and 21, were analyzed using the optical microscope, scanning electron microscope, and energy dispersive x-ray spectroscope. The findings are summarized according to the characterization technique employed.

a.   *Optical Microscopy*

Optical images of both materials seen in Figure 52, looked virtually identical at first glance, but a closer look revealed more dark spots on Sample 21 per area, indicative of higher carbon deposits. Sample 21 contained more urea, the likely source of the greater occurrence of the carbon on the second sample.
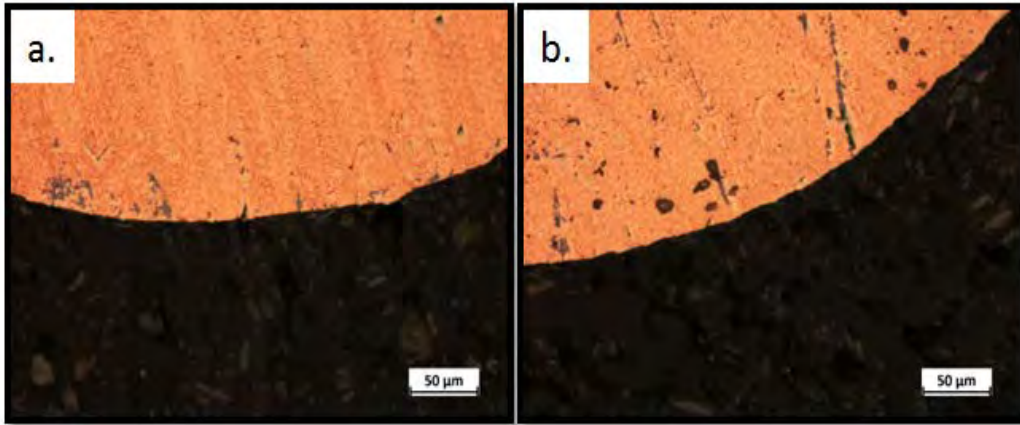
Figure 54.   Optical images of the copper substrates used in (a.) Sample 18 and (b.) Sample 21. Both samples were very similar in appearance, contained dark patches on the surface.

b.   SEM

Characterization of samples using SEM was carried out using secondary electron imaging. In Sample 18 (Figure 53(a.)) the amplified brightness at the outer edge was associated with the ejection of the secondary electrons for the surface. The dark area just inside of the surface edge had a porous appearance. The micrograph of Sample 21 (Figure 53 (b.) was pretty uniform in surface topography.
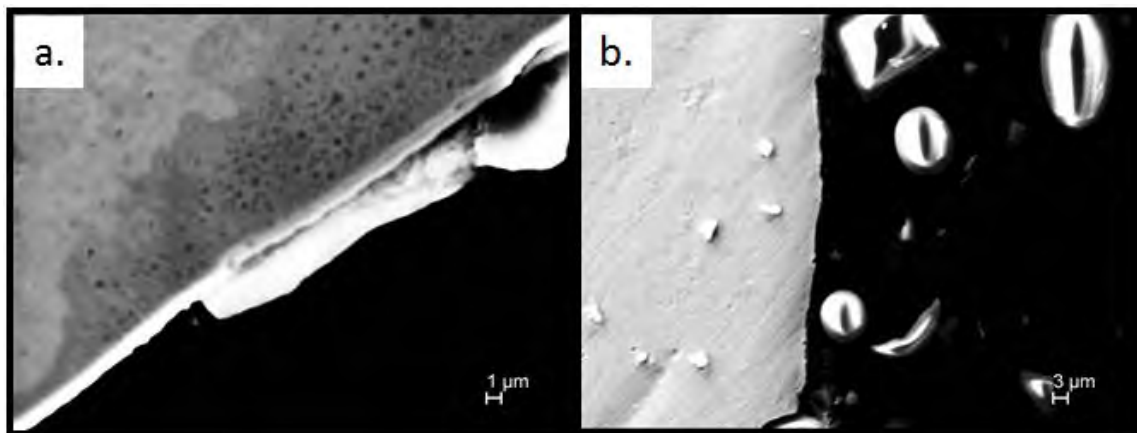
Figure 55.   Secondary electron SEM imaging of (a.) Sample 18 at 1:2:1and (b.) Sample 21 at 1:3:1 of chromium nitrate-urea-Na_2Co_3.

c. ***EDS***

Elemental analysis of both samples provided quantitative results of the material composition after treatment. The EDS spectrum of the outermost edge of Sample 18 is shown in Figure 54 (a.). It contained peaks of carbon and oxygen. The surface of Sample 21 (Figure 54 (b.)), however, had stronger peaks of carbon and oxygen, which was attributed to the higher concentration of urea in the experiment. A small chromium peak was also observed in Sample 21, compared to no deposition of the same element found on Sample 18. No relationship to the findings and the temperature was identified.

Element	At%
CK	23.07
CuK	76.93
Matrix	ZAF

Element	At%
CK	37.95
OK	08.91
CrK	01.95
CuK	51.19
Matrix	ZAF
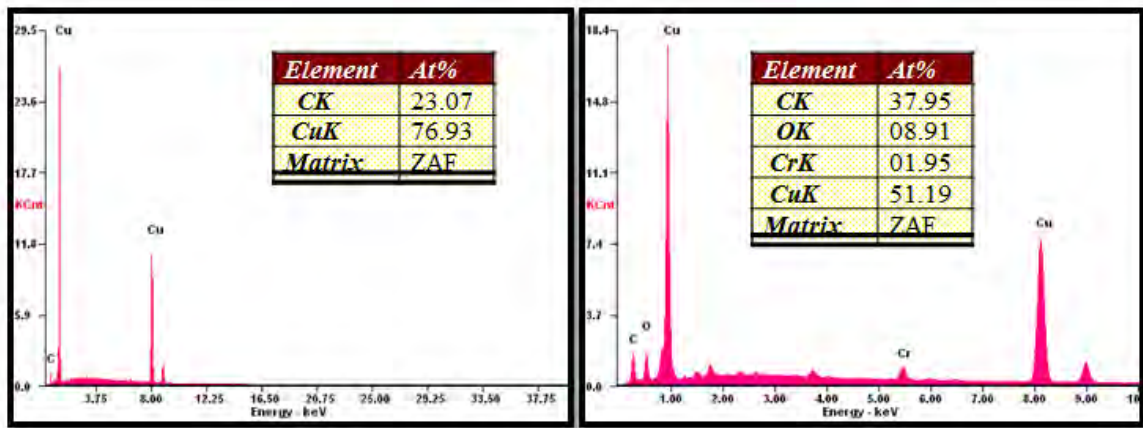
Figure 56.   EDS analysis of the surface of the copper substrates. (a.) Sample 18 (1:2:1) contained less oxygen and carbon when compared to (b.) Sample 21 (1:3:1). Sample 21 also contained limited chromium deposits treatment.

2.   Comparison of Tungsten Substrate

The tungsten substrates used in Samples 19 (1:2:1) and 22 (1:3:1) were subjected to optical microscopy, SEM, and EDS analysis. The results obtained are discussed for each analytical technique used to characterize each sample.

a.   Optical Microscopy

The optical images of Samples 19 and 22 (Figure 55) revealed no distinct coating along the edges of both surfaces despite being treated under varying experimental conditions including urea ratio in the coating mixture and furnace temperature. Additionally, there were no changes to the surface topography or morphology as a result of treatment.
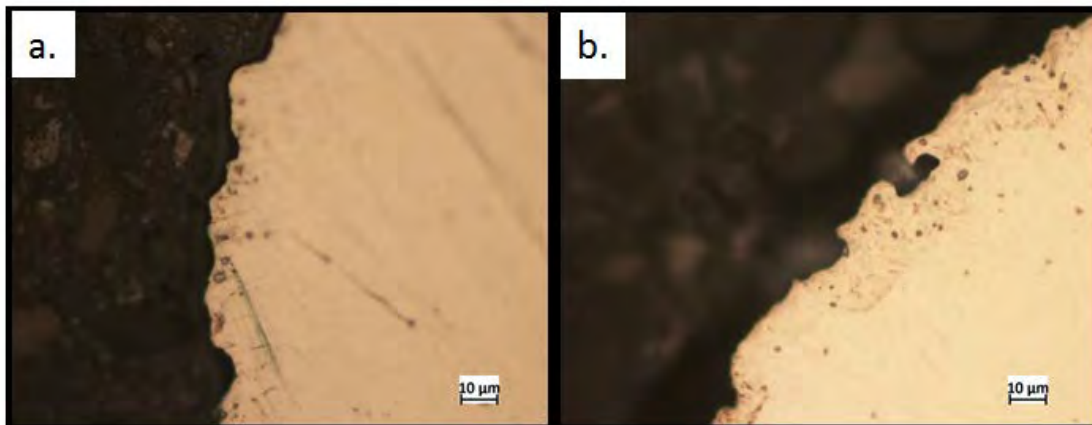
Figure 57.   Optical images of tungsten substrates in (a.) Sample 19 and (b.)
Sample 22. Neither sample showed any distinctive surface layers or
morphological changes after being treated.

b.   *SEM*

SEM imaging of Samples 19 (1:2:1) and 22 (1:3:1) are shown in Figure 56. An
outer layer approximately 22 μm thick was observed along the surface edge of Sample
19. Sample 22, however, did not contain any such features.
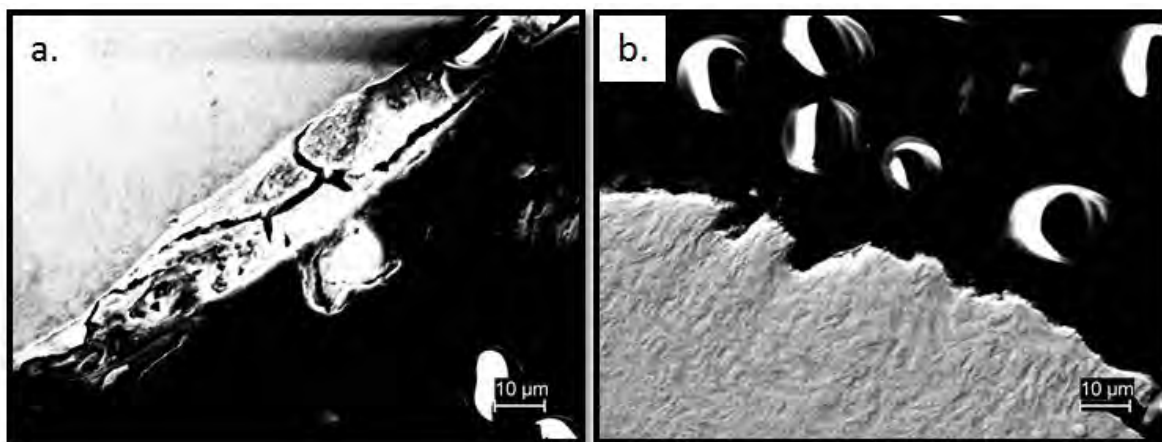
Figure 58.   SEM micrographs of the tungsten substrate in (a.) Sample 19 and
(b.) Sample 22 at 1:2:1 and 1:3:1 ratios, respectively. The formation
of an outer layer was observed in Sample 19. Sample 22 showed no
such outside coating.

c. ***EDS***

Elemental analysis of the Tungsten Samples 19 (1:2:1) and 22 (1:3:1) provided details about the atomic structure that were not apparent with other characterization techniques. The EDS reports of both samples are shown in Figure 59. Oxygen was identified in both samples; however Sample 19 (1:2:1) contained a higher atomic percentage of the oxygen when compared to Sample 22 (1:3:1). The metal-oxide ratio in Sample 19 (1:2:1) was less than 2, which suggesting significant oxidation on the surface. Carbon was also discovered in both samples, with Sample 22 (1:3:1) having essentially a carbon layer on the surface. Chromium deposits were identified in the layer formed in Sample 19 (1:2:1). Sodium was also present in atomic composition of Sample 19. Chromium and sodium were not detected in Sample 22 (1:3:1).
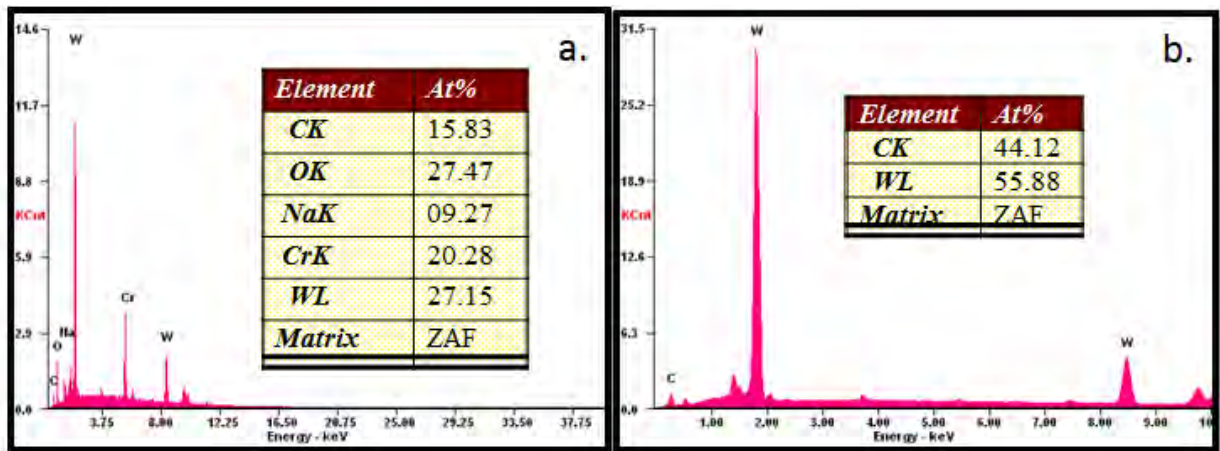
Figure 59.   EDS analysis of (a.) Sample 19 (1:2:1) and (b.) Sample 22 (1:3:1).
Sample 19 contained more carbon and oxygen as compared to
Sample 22. Chromium was discovered in the surface layer of
Sample 19.

3.   Comparison of Stainless Steel Substrates

The stainless steel substrates, Samples 20 (1:2:1) and 23 (1:3:1), were analyzed using the optical microscope, scanning electron microscope, and energy dispersive x-ray spectroscope. The findings are summarized according to the characterization technique employed.

a.   *Optical Microscopy*

Optical images were obtained for both samples as shown in Figure 58. A side-by-side comparison revealed a very distinct surface layer in both samples. A dark trim also lined the outer coating formed in Sample 23 (1:3:1), suggesting a carbon layer. The coating thickness in Sample 20 (1:2:1) was measured at 10 μm. On the contrary, the outer layer in Sample 23 (1:3:1) was determined to be 12 μm. From the surface, it can be concluded that the varied temperature and the urea ratio employed in this analysis did not greatly alter the outcome.
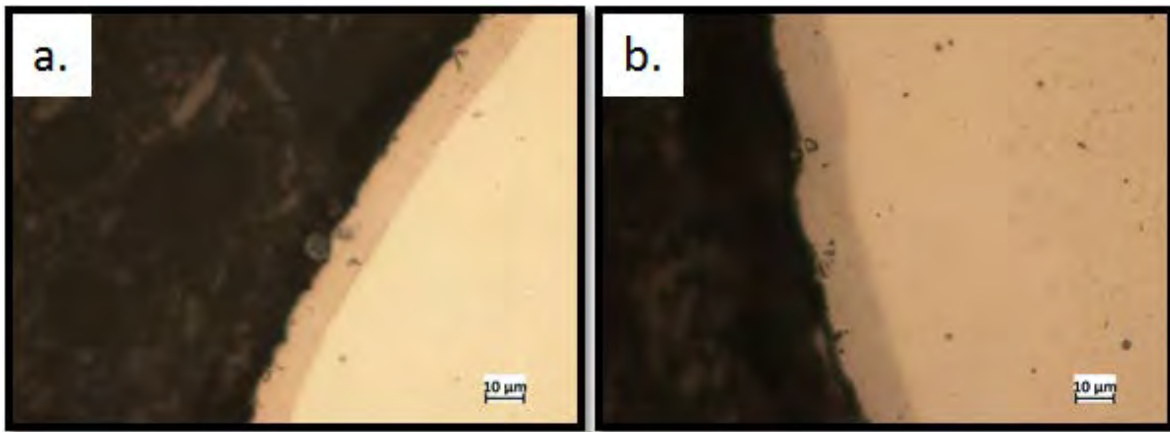
Figure 60.   Optical images of stainless steel substrates in (a.) Sample 20 (1:2:1) and (b.) Sample 23 (1:3:1).

b.   *SEM*

Findings based on the obtained SEM micrographs in Figure 59 supported the altered surface structure observed using optical microscopy. An outer coating was seen on both samples showing a very distinct delineation between the microstructure in the bulk material compared to the outer layers formed.
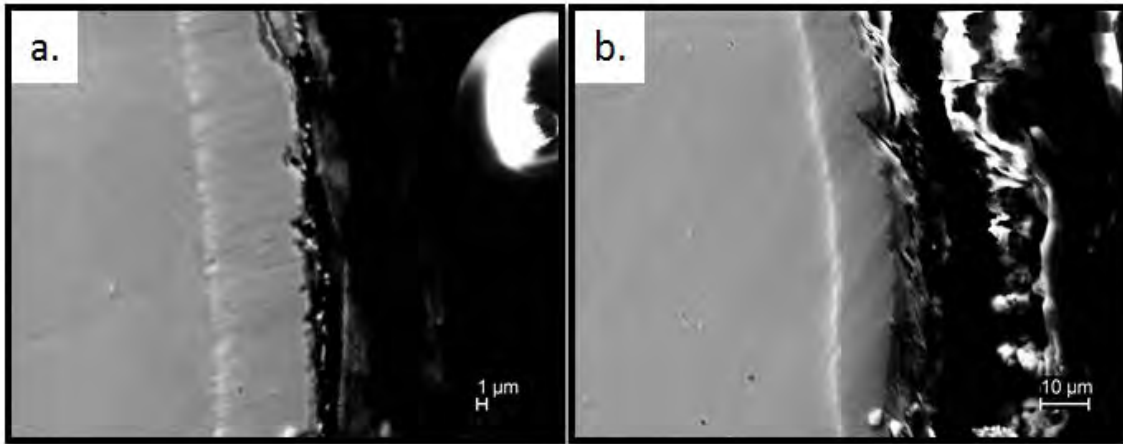
Figure 61. (a.) SEM micrographs of Sample 20 treated with a 1:2:1 coating mixture ratio to 850°C showed an outer layer on the surface. (b.) Sample 23 treated with a 1:3:1 coating mixture ratio to 1000°C showed an outer surface layer.

c. EDS

The elemental composition was taken using EDS spot analysis on the outer layer formed in Samples 20 and 23. The EDS spectrum corresponding to Sample 20 as seen in Figure 60, indicated the deposition of carbon and oxygen on the surface. Quantitative analysis of the same sample suggested little carbon deposited, because the amount measured 6 AT%, is consistent with the bulk material. The metal-oxide ratio was > 6/1, signifying little oxidation. In Sample 23 the presence of high oxidation and carbon levels were indicative of extra urea in the 3:1 ratio with the precursor. Sodium was also detected in the EDS spectrum, leftover from the reagent. The Fe-Cr ratio in Sample 23 was lower compared to the bulk material due to unexpected inter-diffusion of the species during treatment. Both the strong Ca peak and the weak Mg peak were found in the composition of the mounting puck for the samples. One likely explanation for the presence of these elements in the spot analysis is the proximity of the surface edge to the puck, where the analysis was performed.

68
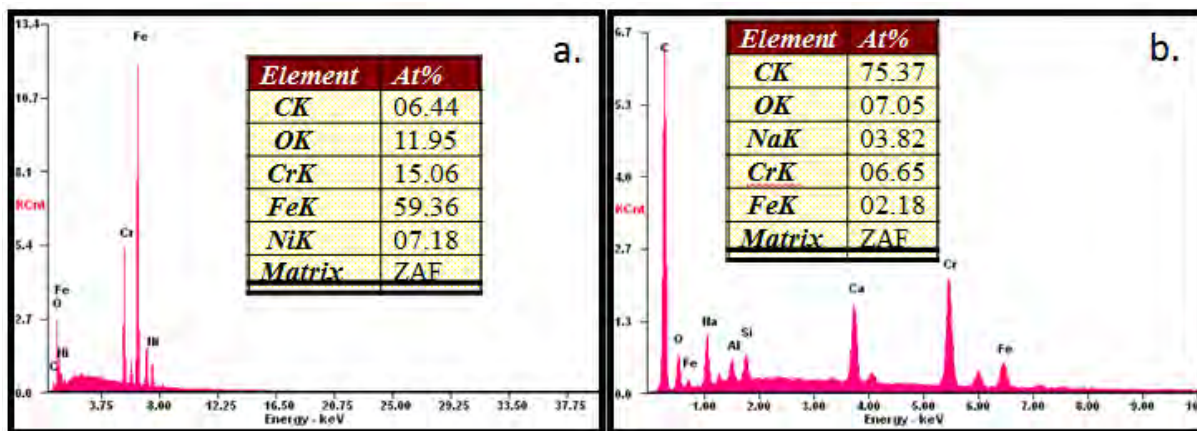
Figure 62.   EDS analysis of the (a.) Sample 20, treated with a 1:2:1 coating mixture and (b.) Sample 23, treated with a coating mixture of 1:3:1. Both samples were employed in the RES-protocol III process.

H.   EFFECT OF PRECURSOR TO REAGENT RATIO

Three stainless steel substrates (Samples 24–26) were treated with the procedure outlined in Protocol III at a temperature of 1000°C but with varying ratios of Na_2CO_3 to determine the impact regarding morphology, topography, and elemental composition of the layer formed. Sample 24 was treated with chromium nitrate-urea-Na_2CO_3 mixture at a ratio of 1:2:1. Sample 25 was treated with 1:2:2 coating mixture ratio. Sample 26 was treated with a 1:2:3 coating mixture ratio. Each sample underwent the same characterization analyses, which included optical microscopy, SEM, and EDS. The findings are discussed according to the technique employed.

1.   Optical Microscopy

Optical microscopy of Samples 24–26 (Figure 61) revealed the formation of an inner and outer surface layer consistent with earlier observations on other stainless steel substrates treated. The coating thicknesses on Sample 24 (1:2:1) were determined to be 8 μm on both the inner and outer layers formed. An inner coating of 5 μm and an outer coating of 11 μm were noted on the surface of Sample 25 (1:2:2). After being treated, Sample 26 (1:2:3) was observed as having an inner layer of 5 μm and an outer layer 8 μm.
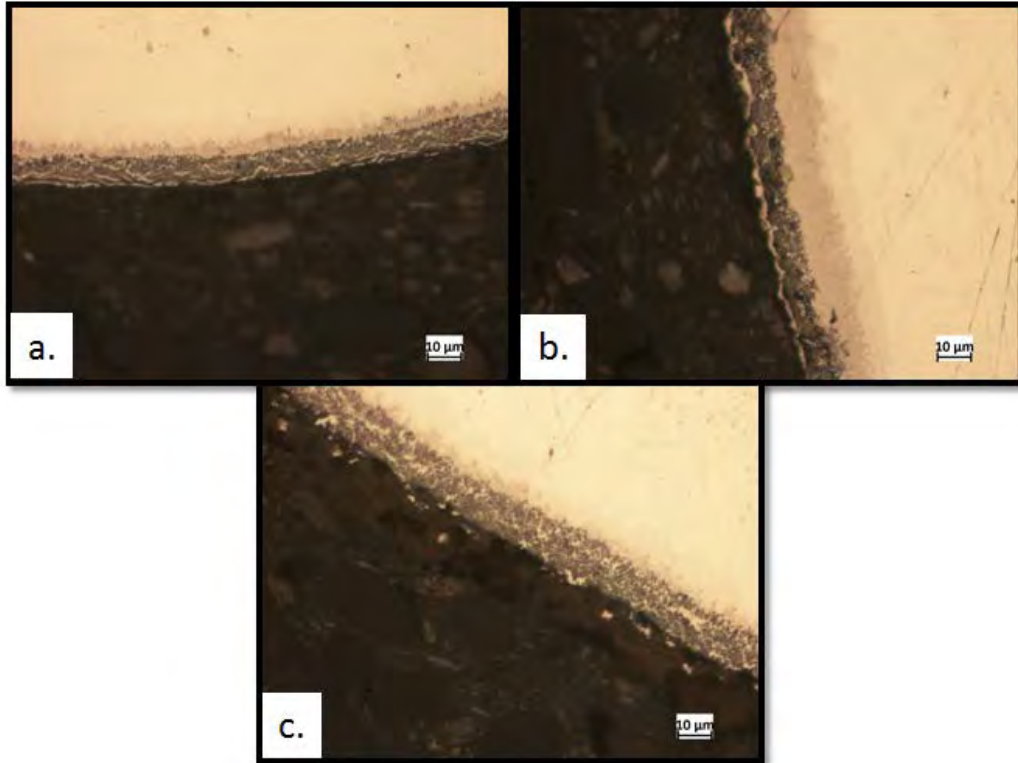
Figure 63.   (a.) Sample 24(stainless steel) at 1:2:1 ratio with chromium nitrate-urea-Na_2CO_3. (b.) Sample 25 (stainless steel) at 1:2:2 ratio of chromium nitrate-urea-Na_2CO_3 (c.) Sample 26 (stainless steel) at 1:2:3 ratio of chromium nitrate- urea-Na_2CO_3.

2.   SEM

The SEM images of Sample 24 (1:2:1), Sample 25 (1:2:2), and Sample 26 (1:2:3) as seen in Figure 62, highlighted changes to the microstructural features on the surface of each the material. In Sample 24 a partial separation or vacancies between the two surface layers was observed. The outermost surface layer in Sample 25 also showed vacancies the outermost layer. The surface layer on Sample 26 was indicative of incomplete fusion between the species.
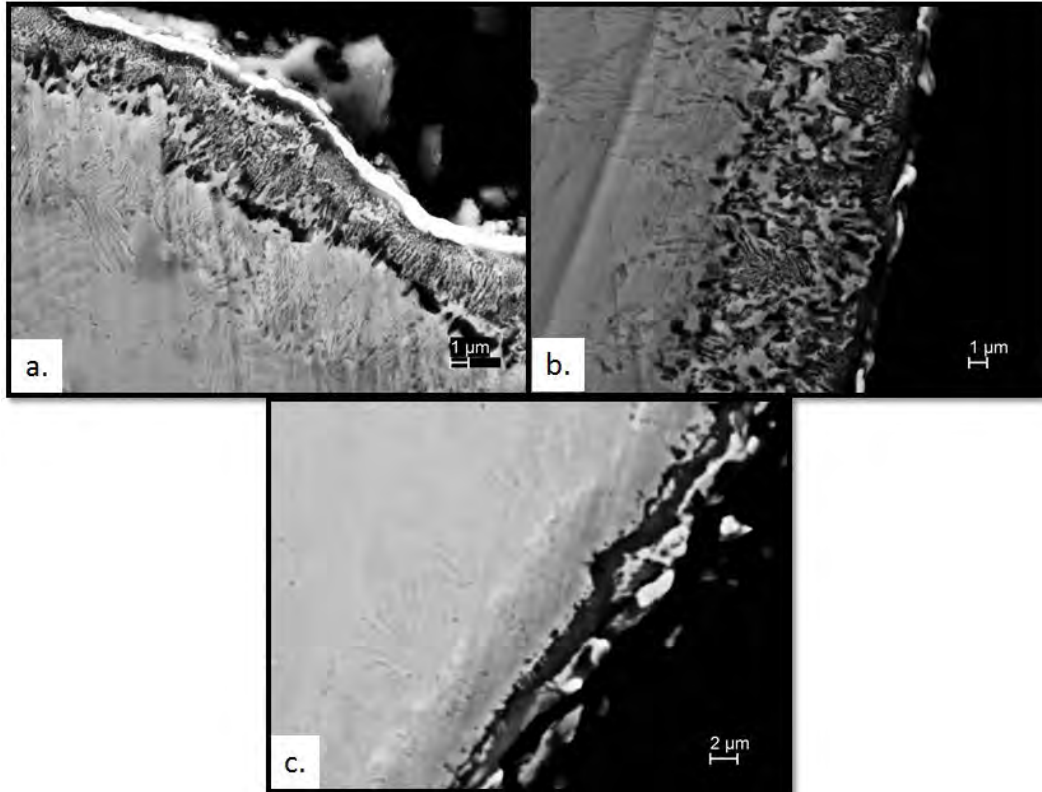
Figure 64.   (a.) SEM image of Samples 24 (stainless steel) treated in a coating mixture of 1:2:1. (b.) SEM image of Sample 25 (stainless steel) treated in a coating mixture of 1:2:2. (c.) SEM image of Sample 26 (stainless steel) treated in a coating mixture of 1:2:3.

a.   EDS

Spot analysis of targeted areas on the surface layers formed during treatment was studied in order to identify the elemental composition of the materials as a result of the varied experimental conditions. Based on the EDS spectrum for Sample 24 as seen in Figure 63 the carbon and oxygen contents were higher in the outer edge compared to the inner layer. Deposits of sodium were also observed on the outer layer in the same sample. These trends relating to the carbon and oxygen levels were consistent for the other samples as evidenced by the EDS spectrums for Sample 25–26 as shown in Figures 64 and 65. In the surface layer of Sample 25, Fe-Cr was observed at 1.5/1 ratio, suggesting chromium enrichment or inter-diffusion of the species during treatment. The surface in Sample 26 was especially peculiar due to a decrease in Fe-Cr to less than 1. Sodium was

also identified in the elemental compositions of the 2 formed layers on Sample 25 and Sample 26 during treatment in order of increasing quantities.

Element	At%
CK	06.46
OK	02.90
NaK	00.00
CrK	16.94
FeK	65.63
NiK	08.08
Matrix	ZAF

Element	At%
CK	15.36
OK	13.02
NaK	05.38
CrK	13.36
FeK	46.37
NiK	06.51
Matrix	ZAF

Figure 65.   EDS spectrums from spot analysis of the (a.) inner layer and (b.) outer layer formed on Sample 24 during treatment in a coating mixture of 1:2:1 at 1000°C.

Element	At%
CK	04.27
OK	15.75
NaK	06.23
CrK	19.29
FeK	48.29
NiK	06.17
Matrix	ZAF

Element	At%
CK	12.68
OK	27.62
NaK	18.25
CrK	15.51
FeK	23.27
NiK	02.67
Matrix	ZAF

Figure 66.   EDS spectrums from spot analysis of the (a.) inner layer and (b.) outer layer formed on Sample 25 during treatment in a coating mixture of 1:2:2 at 1000°C.

Element	At%
CK	09.21
OK	06.34
NaK	03.94
CrK	10.32
FeK	61.25
NiK	08.94
Matrix	ZAF

Element	At%
CK	07.03
OK	22.98
NaK	13.38
CrK	29.84
FeK	23.94
NiK	02.82
Matrix	ZAF
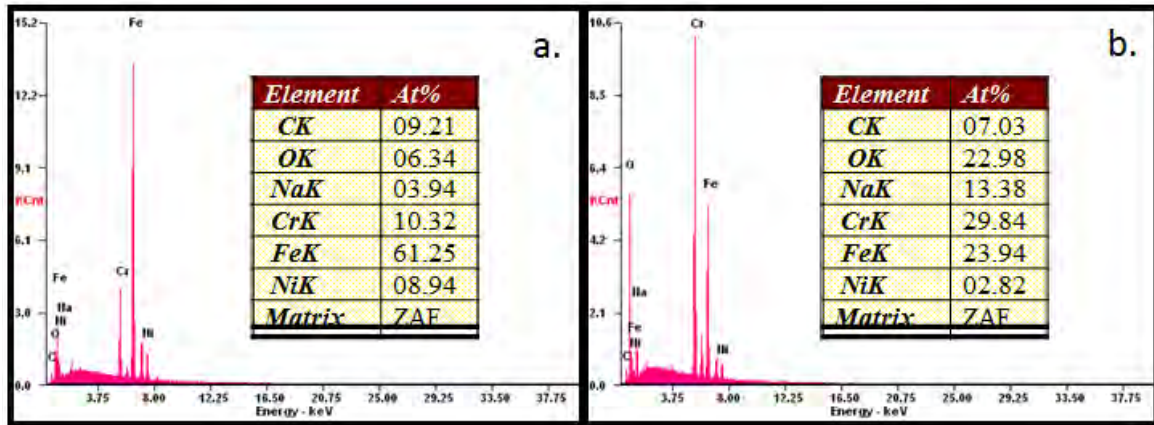
Figure 67.   EDS spectrums from spot analysis of the (a.) inner layer and (b.) outer layer formed on Sample 26 during treatment in a coating mixture of 1:2:3 at 1000°C.

THIS PAGE INTENTIONALLY LEFT BLANK

IV. CONCLUSION

We researched a non-electrolytic process for producing chromium and nickel metal coating as a viable alternative to harmful electrolytic techniques employing hexavalent chromium. The basis of this study was that the RES method for producing submicron particles could be modified to coat macroscopic metal substrates. We performed a series of experiments by rapidly heating different metal substrates in a physical mixture of metal nitrates, urea, and eventually a "carbon combusting" reagent in an inert environment.
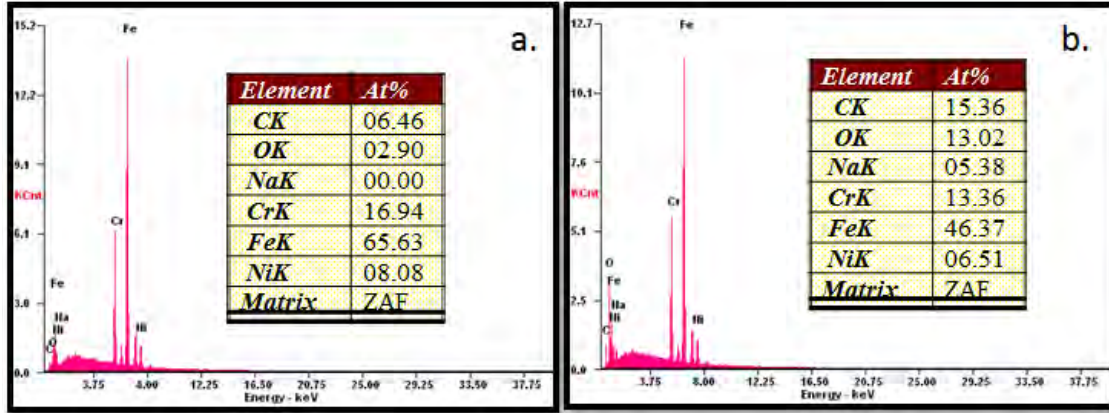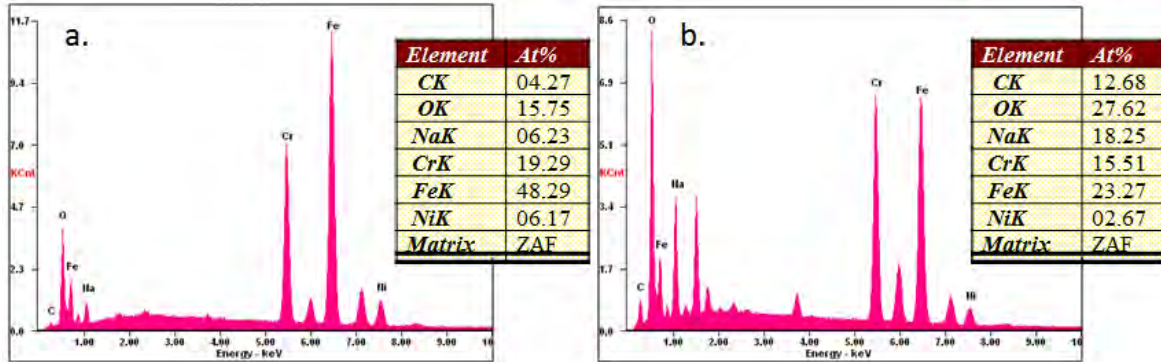
The first protocol demonstrated that a layer could be created on metal surfaces; however, the layer was not pure, and in particular had excess carbon. Another result of the first protocol was the finding that chromium layers form most strongly on steel, and rather poorly on nickel, tungsten, copper and brass. Patches of chrome were found on metals other than steel only. The second protocol introduced a reagent to the coating mixture to limit the presence of carbon and consequently caused only partial decomposition of the additive. The third protocol was designed to both maximize the metal in the surface layer and remove carbon from the deposited layer. Specifically, a "solution" composed of chrome nitrate, urea and sodium carbonate dissolved in ethyl alcohol was used to "paint" a precursor layer directly onto the substrates. No metal was found in the alumina boat post-treatment, suggesting the method did preferentially leave metal in the surface layer. The other objective of the protocol was less successful. The addition of sodium carbonate did lead to minimal carbon in the surface layer but unfortunately, led to the addition of Na to the surface layer from the sodium carbonate. Hence, one impurity was removed, but another added.

During this study, an interesting discovery was made surrounding the use of Na_2CO_3 in the RES Protocol process. We clearly demonstrated that it provided an effective means to burn-off carbon in the surface, and in doing so increased the metal deposit yield on both the stainless steel and copper substrates. Particularly, as we held the temperature constant and increased the ratio of Na_2CO_3 in the coating mixture, we saw a decreasing trend of carbon content. Additionally, inter-diffusion of Fe-Cr boundaries on a

number of the earlier treated stainless steel samples was observed. Na_2CO_3 kept Fe-Cr species from migrating as fast, resulting in a Cr enriched layer.

We also found a preferential pattern for the coating mixtures to interact with selective metals from our batch of samples. Particularly, stainless steel showed tremendous promise after a distinct microstructural change to the surface layer was observed in every trial. Patches of chromium and nickel metal deposition were found on the surface of the copper and tungsten samples but the surfaces were clearly only partially covered. An in-depth analysis of brass metal was not performed to completely rule out its level of success, however, based solely on visual appearance the metal was marginally altered after treatment.

It is unknown how the surface layers formed during analysis have impacted the functional properties of the bulk material. For instance, resistance to corrosion and wear typically go up when a metal object is coating with chromium or nickel. Based on our findings, there were impurities in the coating produced, but even an imperfect coating could have some added benefits. Indeed, it is well known that hard chrome coatings have many "micro cracks". However, in practice this has been found to be an advantage. Lubricants fill these cracks, and apparently enhance the corrosion resistance of the "chrome" layer. Clearly, more research can be done to refine this process. For one, the experimental conditions—temperature, nitrogen gas flow rates, and metal nitrate-urea ratios—employed in this analysis may not have been in the right combination to force more promising results. Secondly, the substitution of the Na_2CO_3 reagent with another, for instance potassium carbonate, may have created a more stable coating structure.

V.   RECOMMENDATIONS FOR FUTURE WORK

There was strong evidence to support our claim that this innovative RES-based process for metal coating yielded partially successful results. First, it is clear that the method created multi-micron thick surface layers of distinct microstructure and composition, particularly on steel. This was substantiated by the resulting elemental composition of the surface layer showing chromium enrichment or deposition in the stainless steel and copper substrates as well as the distinct morphological changes to the surface features in both cases. Indeed, the stainless steel and copper substrates showed the most promise when treated with RES Protocol III however, our analysis did not extend beyond characterization of these materials. It is clear that more work is required in this area in order to better determine the larger impact and efficiency of RES treatment on the samples.

A.   TESTING OF RES PROTOCOL III SURFACE LAYERS

For decades, metal coating has been known to protect the metal substrates against corrosion and enhance the material's mechanical properties. Despite the presence of impurities in our metal coatings produced, no testing of the RES Protocol III surface layers was performed. This measure could provide more in-depth information about the treatment impact. For instance, a corrosion study in which an untreated and treated sample are immersed in a corrosive environment over time then removed and analyzed for metal erosion. Other performance testing criteria can be evaluated to provide more additional changes to the material properties.   For example, how does this process impact hardness, toughness, durability, etc.

B.   EMPLOYING PURE METALS AS SUBSTRATES

Future experiments should be carried out with pure metals. Due to Cr and Ni contained in the bulk stainless steel, it was difficult to predict or fully classify the intermolecular behavior when treated with the mixtures containing either metal nitrate studied. Specifically, inter-diffusion of Fe-Cr during treatment limited the metal deposition yields on the surface. On the contrary, the Cr deposition on the pure copper

wire was easily identified and categorized due to the discrete species involved. Pure Fe wire, for example, would make a viable substrate for Cr or Ni surface overlay because it has a long and proven history as a valuable alloying element with Cr and Ni. Furthermore, it is thermodynamically stable at the operating temperatures employed in this analysis, suggesting metal deposition likely during treatment.

C.   EMPLOYING DIFFERENT REAGENTS

The excess carbon contained in the layer observed in early experiments was inhibited by the addition of Na_2CO_3 to the metal nitrate-urea mixture. After RES Protocol III the elemental contribution of carbon in the localized outer layer was substantially lower than previously observed. The unintended consequence of introducing Na_2CO_3 was the deposition of sodium on the surface due to only partial decomposition of the reagent during treatment. It would be worth exploring other reagents i.e., potassium carbonate (K_2CO_3) and magnesium carbonate ($MgCO_3$) in future steps to remove impurities and fully decompose without a trace.

D.   LOWER TEMPERATURE

The presence of oxygen in the surface layer was attributed to the breakdown of the NOx groups in the nitrate at the high temperature (1000°C) employed in RES Protocol III. Urea undergoes thermal decomposition at roughly 550°C. Therefore, it is expected that by lowering the temperature there will be less breakdown of the NOx groups during treatment. If the temperature is too low, however, it is likely that the chemistry will not take place fully. The optimum temperature for future works is possibly in the range of 600–850°C.

E.   INCREASE NITROGEN FLOWRATES

During treatment, the nitrogen gas flowrate was set to 10 sccm. This slow rate is believed to have led to the formation of carbon monoxide (CO) and ammonia (NH_3) gas as urea decomposed. The CO contributed to the carbon deposited on the substrate surface, while the nitrogen in the ammonia led to nitrides and the nitrogen identified in through elemental analysis portion of the experiments. By increasing the flowrate, the

radicals produced during decomposition of the urea will not be able deposit on the substrate, but instead will be pushed out of the system through the discharge end of the quartz tube.

It may also be advisable to substitute argon for nitrogen. There was some evidence of nitrogen reacting with the substrates.

THIS PAGE INTENTIONALLY LEFT BLANK

LIST OF REFERENCES

[1]   J. Colaruotolo and D. Tramontana, "Engineering applications of electroless nickel," *Electroless Plating: Fundamentals and Applications.* Glen O. Mallory and Juan B. Hadju, Eds., Norwich, NY: Noyes Publications/William Andrew Publishing, 1990, pp 207–227.

[2]   R. A. Lane, C. Fink, C. Grethlein and N. Rome. "Analysis of alternatives to hexavalent chromium: A program management guide to minimize the use of CrVI in military systems," *AMMTIAC-WSTIA,* vol. 1, no. 2, pp. 3–9, Sept. 2012.

[3]   K. Legg, M. Graham, P. Chang, F. Rastagar, A. Gonzales and B. Sartwell, "The replacement of electroplating," *Surf. Coat. Technol.,* vol. 81, pp. 99–105, May 1996.

[4]   N. Patton. (2014, Jul. 17). Greener Hard Chromium Plating. *Products Finishing* [Online]. Available: http://www.pfonline.com/articles/greener-hard-chromium-plating

[5]   V. S. Protsenko and F. I. Danilov, "Chromium electroplating from trivalent chromium baths as an environmentally friendly alternative to hazardous hexavalent chromium baths: comparative study on advantages and disadvantages," *Clean Technol. Envir.,* vol. 16, pp. 1201–1206, Aug. 2014.

[6]   G. M. Ingo, G. Guida, E. Angelini, G. Di Carlo, A. Mezzi and G. Padeletti, "Ancient mercury-based plating methods: combined use of surface analytical techniques for the study of manufacturing process and degradation phenomena," *Acc. Chem. Res.,* vol. 46, pp. 2365–2375, 2013.

[7]   Metal coatings. (2002, Nov. 15) *Machine Design.* [Online]. Available: http://machinedesign.com/basics-design/metal-coatings.

[8]   L. Frazer. (2006, Aug.). Shiny science - A new substitute for hexavalent chromium. *Environ. Health Perspect.* [Online]. Volume 114(8). pp. A482-A485. Available: http://www.ncbi.nlm.nih.gov/pmc/articles/PMC1552031/

[9]   H. H. Lou and Y. Huang, "Electroplating," in *Encyclopedia of Chemical Processing,* S. Lee (ed.), Marcel Dekker, Ed. New York, NY: Taylor and Francis Group, 2007.

[10]   B. Sartwell. (2009, Jan. 13). Replacement of Hexavalent Chromium on DOD Weapons Systems. [Online]. Available: http://www.denix.osd.mil/cmrmd/ECMR/HexChrome/DODRiskManagement.cfm

[11]   I. Rose and C. Whittington. (2014, Jun. 17). *Nickel Plating Handbook.* Nickel
        Institute Brussels, Belgium. [Online]. Available: http://www.nickelinstitute.org

[12]   G. A. Di Bari, "Electrodeposition of nickel," in *Modern Electroplating,* vol. 5, M.
        Schlesinger and M. Paunovic, Eds., 5th ed. Hoboken, New Jersey: John Wiley
        and Sons, Inc., 2010, pp 79–114.

[13]   M. Schlesinger, "Electroless deposition of nickel," in *Modern Electroplating,* vol.
        4, M. Schlesinger and M. Paunovic, Eds., 5th ed. Hoboken, NJ: John Wiley and
        Sons, Inc., 2010, pp. 667–684.

[14]   R. Parkinson, "Properties and applications of electroless nickel," *Nickel
        Development Institute*, 1997.

[15]   P. Benaben. (2011, Jan. 31) An overview of hard chromium plating using trivalent
        chromium solutions," *Products Finishing,* [Online]. Available:
        http://www.pfonline.com/articles/an-overview-of-hard-chromium-plating-using-
        trivalent-chromium-solutions

[16]   K. Wasa and S. Hayakewa, *Handbook of Sputter Deposition,* 2nd ed. New Jersey:
        Noyes Publications, 1992.

[17]   Physical Vapor Deposition (PVD). [Online]. Available:
        http://www.sigmaaldrich.com/materials-science/material-science-
        products.html?TablePage=108832720. Accessed May 1, 2015.

[18]   C. Reeve, (2001, Nov. 22). Thermal spray: better performance for less. *Machine
        Design* [Online]. Available: http://machinedesign.com/archive/thermal-spray-
        better-performance-less.

[19]   A. Vardelle, C. Moreau, N. J. Themelis and C. Chazelas. (2014, Dec. 11). A
        Perspective on Plasma Spray Technology. *Plasma Chem. Plasma
        Process.,*[Online]. pp. 1–19, Available:
        http://www.seas.columbia.edu/earth/wtert/sofos/Plasma_%20spraying_Nov2014.
        pdf.

[20]   R. J. Molz and R. J. McCullough. "Better performance of plasma thermal spray."
        Sulzer Tech. Rev., vol. 88, pp. 12–13, Feb. 2006.

[21]   P. Bright, P. S. Burge, S. P. O'Hickey, P. F. Gannon, A. S. Robertson and A.
        Boran, "Occupational asthma due to chrome and nickel electroplating," *Thorax,*
        vol. 52, pp. 28–32, Jan. 1997.

[22]   M. Costa, "Potential hazards of hexavalent chromate in our drinking water,"
        Toxicol. Appl. Pharmacol., vol. 188, pp. 1–5, 2003.

[23]   C. Pellerin and S. M. Booker, "Reflections on hexavalent chromium: health hazards of an industrial heavyweight," *Environ. Health Perspect.,* vol. 108, pp. A402-7, Sep. 2000.

[24]   E. F. Herzberg, N. T. O'Meara and R. F. Stroh. (2015, Mar.). The Annual Cost of Corrosion for Cost Guard Aviation and Vessels. LMI. [Online]. Available: http://www.corrconnect.org/eblast/2015_may/CoastGuardCostofCorrosion_Aviati onVessels_summary.pdf.

[25]   Department of Defense, Memorandum: "Minimizing the Use of Hexavalent Chromium (Cr^6+)," Under Secretary of Defense (AT&L), Washington, DC, 2009.

[26]   C. A. Huang, C. Y. Chen, C. C. Chen, T. Kelly and H. M. Lin, "Microstructure analysis of a Cr-Ni multilayer pulse-electroplated in a bath containing trivalent chromium and divalent nickel ions," *Surf. Coat. Technol.,* vol. 255, pp. 153–157, Sep. 2014.

[27]   S. C. Kwon, A. Kim, S. U. Park, D. Y. Kim, D. Kim, K. S. Nam and Y. Choi, "Characterization of intermediate Cr-C layer fabricated by electrodeposition in hexavalent and trivalent chromium baths," *Surf. Coat. Technol.,* vol. 183, pp. 151–156, May 2004,

[28]   S. Mohan, G. Saravanan and N. G. Renganathan, "Comparison of chromium coatings and electrochemical behavior with direct current and pulse current deposition in trivalent chromium formate urea bath as alternative to conventional Cr coatings," *Surface Engineering,* vol. 27, pp. 775–783, Nov. 2011.

[29]   Y. B. Song and D. T. Chin, "Current efficiency and polarization behavior of trivalent chromium electrodeposition process," *Electrochim. Acta,* vol. 48, pp. 349–356, Dec. 2002.

[30]   Z. Zeng, L. Wang, A. Liang and J. Zhang, "Tribological and electrochemical behavior of thick Cr-C alloy coatings electrodeposited in trivalent chromium bath as an alternative to conventional Cr coatings," *Electrochim. Acta,* vol. 52, pp. 1366–1373, Nov. 2006.

[31]   J. D. Schell and M. Rechtsteiner, "Replacement of chromium electroplating using advanced material technologies on gas turbine engine components," *Plating and Surface Finishing,* vol. 87, pp. 17–23, 2000.

[32]   C. Luhrs, M. Kane, Z. Leseman and J. Phillips, "Novel Process for Solid State Reduction of Metal Oxides and Hydroxides," *Metallurgical and Materials*

Transactions B-Process Metallurgy and Materials Processing Science, vol. 44, pp. 115–122, Feb. 2013.

[33]   H. Zea, C. C. Luhrs and J. Phillips, "Reductive/expansion synthesis of zero valent submicron and nanometal particles," *J. Mater. Res.,* vol. 26, pp. 672–681, Mar. 2011, 2011.

[34]   M. Bai, S. Zhao and S. Asuha, "Synthesis and thermal decomposition of Cr–urea complex," *Journal of Thermal Analysis and Calorimetry,* vol. 115, pp. 255–258, 2014.

[35]   A. S. Gow III and J. Phillips, "Microcalorimetric study of oxygen adsorption on catalytically promoted gasification chars: mechanistic evidence for alkali-and alkaline-earth-metal carbonate catalyzed reactions," *Energy Fuels,* vol. 6, pp. 526–532, 1992.

[36]   C. Mims, J. Chludzinski, J. Pabst and R. Baker, "Potassium-catalyzed gasification of graphite in oxygen and steam," *Journal of Catalysis,* vol. 88, pp. 97–106, 1984.

[37]   C. A. Mims and J. K. Pabst, "Alkali catalyzed carbon gasification I. Nature of the catalytic sites," *Preprints—American Chemical Society, Division of Petroleum Chemistry,* vol. 180, pp. 258–262, 1980.

[38]   C. A. Mims and J. K. Pabst, "Role of surface salt complexes in alkali-catalysed carbon gasification," *Fuel,* vol. 62, pp. 176–179, 1983.

INITIAL DISTRIBUTION LIST

1.   Defense Technical Information Center
        Ft. Belvoir, Virginia

2.   Dudley Knox Library
        Naval Postgraduate School
        Monterey, California